THE EVALUATION OF CIRCUIT MODELS OF LUMPED PASSIVE FLUIDIC COMPONENTS

By

JOSEPH MORTON ISEMAN

Bachelor of Science
George Washington University
Washington, D. C.
1961

Master of Science in Engineering
The Catholic University of America
Washington, D. C.
1969

Submitted to the Faculty of the Graduate College
of the Oklahoma State University
in partial fulfillment of the requirements
of the Degree of
DOCTOR OF PHILOSOPHY
May, 1976

THE EVALUATION OF CIRCUIT MODELS OF LUMPED

PASSIVE FLUIDIC COMPONENTS

Thesis Approved:

Karl M. Reid

Thesis Adviser

R L Lowery

W. A. Tiedeman

Wayne Yarbrough

Robert J. Mulholland

N N Durham

Dean of the Graduate College

PREFACE

This study was geared toward tying together voluminous research studies on passive fluidic components so that they can be used more directly and with greater understanding in the design of fluidic hardware. The primary objectives were to develop an algorithm for evaluating equivalent circuit models of passive fluidic components; to synthesize circuit models from the best models in the literature; and to develop a user-oriented fluidic circuit analysis code.

I am greatly indebted to my major adviser, Dr. Karl N. Reid, Jr., for bringing me into the doctoral program and giving me continuing guidance and inspiration in this study over the miles and over the years. Special appreciation is due to Joseph M. Kirshner, Chief of the Fluidic Systems Research Branch, Harry Diamond Laboratories for his continuing encouragement and patience. A debt of gratitude must be expressed to the Harry Diamond Laboratories, U.S. Army Materiel Command, for total financial support of this research effort.

Appreciation is also expressed to the other committee members: Dr. Richard L. Lowery, Dr. Robert J. Mulholland, Dr. William G. Tiederman, Jr., and Dr. Radha K. Yarlagadda for continuing interest and helpful suggestions in bringing this thesis into final form.

No words are sufficient to express the thanks to my loving and loveable wife Sheila who has been the constant reminder of a reason to finish a lengthy graduate program. To my mother, Lucile V. Iseman, and to my father, Isaac Iseman (deceased), I have always said thank you for

showing me the way.

To my many friends and colleagues at the Harry Diamond Laboratories and at Oklahoma State University, I offer another thank you for their constant encouragement and helpful discussions. Not trying to cite all or omit any, I wish to thank Hobie Audet, Dr. Marvin M. Cohen, Richard Deadwyler, Ted Drzewiecki, Dr. Norman A. Eisenberg (who ably reviewed this dissertation), Albert Freiling, Maurice Funke, John M. Goto, Arthur Hausner, Dr. Silas Katz, Allan F. Malmberg, Francis M. Manion, Dr. George Mon, Arthur J. Ostdiek, Robert Puttcamp, Harold Robinson, Gary L. Roffman, Robert Talbot, Kenji Toda, Dyrull V. White, and Dr. Robert Woods.

Thanks also is given to typists Dawn D. Perry, Ercelle Janifer, Sarah O'Brien, Deanna Patterson, Kay Mays, and Linda Howard.

TABLE OF CONTENTS

LIST OF TABLES

LIST OF FIGURES

NOMENCLATURE

a	acoustic velocity (m/sec)
a_∞	ambient acoustic velocity (m/sec)
A	area (m^2)
C	capacitance (m^4-sec^2/kg)
C_p	specific heat capacity at constant pressure ($m^2/sec\,^oC$)
d	diameter (m)
$D(\omega)$	freqeuncy dependent energy dissipation (kg/m^4 -sec)
E	error (-)
f	number of circuit elements described by frequency dependent parameters (-)
F	friction coefficient (-)
G	magnitude ratio, or gain (-)
i	current (amperes)
k	spring constant (kg/m^2-sec^2)
ℓ	length (m)
L	inductance (inertance) (kg/m^4)
n	number of circuit elements described by nonlinear parameters (-)
n	polytropic coefficient (-)
N	number of circuit elements in lumped circuit model (-)
N	number of passages in a capillary module (-)
N_R	Reynolds number $N_R = (\frac{u}{\nu})$ x (characteristic dimension)
p	gauge static pressure (Pa)

NOMENCLATURE (Continued)

P	Laplace transform of static pressure (Pa/sec)
$\dot{p}$	time rate of change of static pressure (Pa/sec)
p_a	absolute static pressure (Pa)
p_{21}	pressure drop (Pa)
p_∞	ambient or reference pressure (Pa)
Q	volume flow (m^3/sec)
r	radius (m)
R	resistance (kg/m^4sec)
s	Laplace variable (1/sec)
s	number of segments in method of characteristics solution (-)
t	time (sec)
u	particle velocity (m/sec)
v	voltage (volts)
V	volume (m^3)
X_C	capacitive reactance (kg/m^4-sec)
X_L	inductive reactance (kg/m^4-sec)
y	state variable

Greek Symbols

α	$r\left(\frac{\omega\rho C_p}{\kappa}\right)^{\frac{1}{2}}$ (defined in equation (3.18c) (-)
γ	ratio of specific heats (-)
ζ	damping ratio (kg/m^4)

NOMENCLATURE (Continued)

κ	thermal conductivity (kg m/sec^2- ^oC)
λ	factor in inertance (-)
μ	absolute viscosity (kg/m-sec)
ν	kinematic viscosity (m^2/sec)
ρ	mass density (kg/m^3)
ρ_∞	ambient mass density (kg/m^3)
τ	time constant (sec)
ω	radian frequency (1/sec)
ω_n	undamped natural frequency (1/sec)

Subscripts

calc	calculated
char	characteristic
db	decibel, e.g., G_{db}
i	input
ℓ	linear
L	load
LB	left boundary
m	model to be evaluated
max	maximum
meas	measured
N	nonlinear
o	output

NOMENCLATURE (Continued)

q	flow dependent
r	reference model
ref	reference model
RB	right boundary
seg	spatial segment
ss	steady state

CHAPTER I

INTRODUCTION

Background

A fluidic system is a physical array of interconnected components. Typical fluidic systems include passive components (capillaries, orifices, tanks and other enclosed volumes, bellows, diaphragms, lines, transmission lines, junctions, area changes, and passive sensors) and active components (fluid amplifiers and active sensors). A goal in fluidic systems analysis is the formulation of a mathematical model which describes the essential steady state and dynamic behavior of the system. The system model is an interconnected group of component models. Generally, a set of models of varying complexity, validity and applicability may be identified for each physical component. From each set the best component model is evaluated as the simplest one which provides the information required for given engineering action. The modeling process discussed in this thesis includes both the formulation and evaluation of models of fluidic components.

Component models may be formulated from 1) basic principles of physics (internal flow field approach; references 1 through 8), 2) an experimental analysis (black box approach; references 9 and 10), or 3) a combination of the two.

In the internal flow field approach, governing equations represent detailed internal fluid phenomena including potential flow, viscous

flow, acoustics, gas dynamics, or jet flow in terms of internal fluid variables. In the black-box approach each component model represents internal fluid processes, measured only in terms of external terminal variables.

Fluid governing equations which describe the fluid motion within a given component are rarely easy to solve. However, by applying appropriate simplifying approximations both to the equations and to the boundary conditions, a set of governing equations for a particular process can sometimes be replaced by a set of algebraic and/or differential equations which are more conveniently solved. Solutions to these equations also describe the essential internal processes, but do so in terms of measurable external terminal variables.

In fluidic systems the fundamental governing equations often are partial differential equations (in terms of only one independent spatial variable) representing distributed parameter models. These equations often can be restated as ordinary differential equations representing lumped (rather than distributed) parameter models (reference 11). Ordinary differential equations transfer directly into equivalent circuit models -- topological structures of pure circuit elements which mathematically relate the terminal variables -- static pressure and flow rate. These equivalent circuit models (reference 12) are analogous to the circuit models used in electronics and several other technical fields such as heat transfer, mechanics, hydraulics, and pneumatics. Analyses, based on equivalent circuit models, are relatively simple to perform and are often of sufficient accuracy to demonstrate the essential behavior or fluidic systems. Hereafter the terms "equivalent circuit models" and "circuit models" are used interchangeably.

The digital computer simulation of linear equivalent circuit models is usually simple and straightforward. This simplicity occurs because analytical techniques, which have been developed to a high degree of sophistication for electronic circuits, can be applied equally well to analogous forms of fluidic equivalent circuits.

However, there are difficulties in readily representing unique properties of physical fluidic components in terms of circuit models. Despite the rather extensive literature in fluidics (e.g., see reference 13), very little effort has been expended to develop consistent models for fluidic components. The available models cover different dynamic ranges and different bandwidths and have different degrees of precision.

Circuit models of fluidic components may include nonlinear elements with frequency dependent parameters. Viewed in terms of topological structure, they are natural extensions of linear, frequency independent fluidic component models. Viewed in terms of digital computer programs, some techniques (which generally are not available in standard digital programs for electronic circuits) must be appended to these programs to permit both steady state and dynamic response calculations.

Once the circuit models for a particular component are identified, collected, and organized, an evaluation procedure is needed: 1) to determine the adequacy of the models over the operating ranges of interest, and 2) to indicate the "best" equivalent circuit model to use in a particular application. It may be possible to conceive of or to identify a model which covers the operating range of interest with more than enough accuracy. Such a model can serve as a reference by which all other models can be compared.

Boyle et al. (reference 14) indicate that digital computer

optimizations of electronic systems, using the most complex circuit models, may be totally uneconomical. An identical concern over cost in fluidic system optimizations is expressed by this author. It is therefore appropriate that a model evaluation process penalize the cost of added model complexity. An ad hoc penalty function can be envisioned for including some measure of added expense in developing and utilizing equivalent circuit models of varying degrees of complexity.

Objectives

The fluidic systems analyst faces a dilemma as to which component model to select from an available or derivable set for each physical component in a systems application. Sensitivity of system behavior to changes in a component model may be large or small. A model which is appropriate in one case may be more or less than adequate in another. Generally, the goal is selection of the simplest model that will fulfill the engineering need in the analysis of a particular system. There are, however, tradeoffs which exist between model accuracy and digital simulation costs that have been difficult to quantify. Also, it is generally agreed that analytical design of fluidic systems has been hampered by the lack of general purpose, user-oriented digital simulation programs comparable to those used in electronic circuit analysis. If precise simulation results which can easily be interpreted by an engineer are required, then simultaneous instead of computationally delayed solutions are virtually imperative for other than linear d-c or small signal a-c analyses.

Thus the following three principal objectives were established for this thesis study:

1. To develop for a given passive fluidic component, a quantitative procedure for selecting the "best" equivalent circuit model which is based upon a validated reference model and a user-chosen "cost" or "penalty" function.
2. To adapt two existing circuit analysis programs (NET-2 and SLIC) for use in the simulation of passive fluidic systems.
3. To develop a general approach to the analytical design of passive fluidic systems.

Thesis Outline

This thesis defines an approach for the formulation and evaluation of equivalent circuit models for passive fluidic components, demonstrates the use of some of the circuit models in the study of several typical passive networks, and describes a possible strategy for designing physical fluidic systems.

Chapter II sets a perspective for the basic part of the study by defining a circuit model formulation procedure through which energy dissipation and energy storage processes are represented in terms of pure fluid circuit elements (see reference 12). A model evaluation algorithm is proposed for calculating steady state and dynamic errors of equivalent circuit models with respect to a reference model and in terms of a user-chosen penalty function. Methods are outlined for performing steady state and dynamic response measurements to verify the computed responses of the reference models.

In Chapter III, circuit models are selected for a capillary module, an enclosed volume, and a bellows module. The model evaluation procedure is demonstrated using transient (pressure step) signals for

1. a component with an essentially steady state process -- the capillary module -- loaded by a second capillary module and
2. a component with an essentially dynamic process -- a tank (enclosed volume) -- in a three component test configuration including two capillary modules.

Lumped parameter models of the tank (enclosed volume) and both lumped and distributed parameter models of the capillary module are first formulated and then simulated for the overall systems model. Evaluation of component models is made on the basis of phase plane pressure trajectory plots ($\dot{p}$ vs p).

Chapter IV outlines considerations in selecting a digital simulation program:

1. which can be adapted for use with simple and complex fluidic circuit models and
2. which is strongly user-oriented.

Both SLIC and NET-2 have been adapted for fluidic systems simulation as a part of this thesis effort. Of the two programs, NET-2 has far greater versatility.

Although circuit models of capillary modules and tanks can be evaluated in simple configurations from the viewpoint of time domain analysis, hardware specifications for a fluidic system often are presented in terms of frequency domain analysis. The use of equivalent circuit models (formulated in Chapter III) for certain fluidic components is illustrated in the study of a passive summing junction and a passive lead compensation network in Chapter V. The studies performed in Chapter V may be viewed as an alternative model evaluation or verification procedure using small signal a-c signals in larger systems

models (networks) than in Chapter III. Evaluation of component models in several systems models is made from frequency-dependent pressure response plots (Bode plots -- pressure magnitude versus radian frequency and pressure phase difference versus radian frequency).

A method is suggested in Chapter VI for proceeding directly from desired behavior or specifications to optimum selection of geometric parameters of physical fluidic components.

Summary

A circuit model evaluation procedure has been defined. The evaluation algorithm involves comparing the computed steady state and transient dynamic response of each model under consideration with that of an experimentally validated reference model. Steady state and dynamic errors are determined for the terminal variables, presented as phase-plane plots. Ad hoc quantitative penalty factors are used as multipliers of the steady state and dynamic errors to give penalized steady state and dynamic errors. The results tend to confirm that a trade-off exists between model complexity and model cost. That is, the "best" component model to use in a system analysis may not be the one which most closely represents the actual behavior of the component.

Several equivalent circuit-based digital simulation programs were evaluated. It is demonstrated that if a computer with sufficient memory is available, the utility of each program is directly related to the cost of:

1. revising available software,
2. formulating problems in terms of generalized ordinary differential equations,

3. entering a circuit model into the input format of the computer program (usually of small cost), and
4. making computer simulation runs (usually the most significant cost).

As an alternative to evaluating a component model by its transient dynamic response in Chapter III, Bode frequency response is considered in Chapter V. Bode plots of various component models are calculated and compared to physical response data in terms of magnitude and phase difference. These results indicate (as in the more formal evaluation procedures which are discussed in Chapter II and implemented in Chapter III) that there is a trade-off between model complexity and modeling costs.

Finally, an approach is outlined for choosing optimum parameters in equivalent circuits in the computer-aided design of fluidic networks and systems.

Conclusions and Recommendations

An evaluation algorithm has been demonstrated to have both qualitative and quantitative significance for assessing validity of sets of equivalent circuit models of passive fluidic components with respect to a reference model. It is concluded that a "best" model must be somewhat subjective because of specifications set forth by the user of the evaluation algorithm on a set of models, on a reference model, on a set of test conditions, and on error criteria for trading off model sophistication against modeling cost.

It is further concluded that an equivalent circuit model, although not always predicting response exactly for a physical component, can be

evaluated as "best" in the sense of being the most adequate model. The evaluation procedure was demonstrated to have validity for two specific devices -- a capillary module and a tank -- with typical but specialized signal and load conditions. This evaluation procedure should be applied to other fluidic components and more extensively to the capillary module and the tank. It is also recommended that alternate evaluation algorithms should be hypothesized and verified for relevance in selecting a "best" model in a given network specification.

Although this evaluation algorithm was demonstrated specifically for responses in the time domain, it is felt that an alternate procedure, based on frequency response, can equally well validate a "best" component model, at least in the sense of linear dynamic effects.

Finally, it is concluded that it is extremely important for programming structures with a maximum degree of user ease and flexibility to be applied to computer-aided design based on equivalent circuit models.

CHAPTER II

CIRCUIT MODEL FORMULATION AND EVALUATION

An underlying question in dynamic system modeling, analysis and design is, "What is the simplest circuit model which will give adequate results relative to a physical component in a real system?" This question was raised by Lindholm and Director (reference 15) and by Happ and Staudhammer (reference 16) in attempting to assess the adequacy of models of semiconductor devices in the analysis of electronic integrated circuits.

Lindholm and Director (reference 15) simulated large-scale semiconductor circuits using various equivalent circuit models for each semiconductor device. The evaluation technique employed a digital computer to crank through computations in searching for voltage and current responses which were self-consistent with assumptions of the component models. Happ and Staudhammer (reference 16) performed an order of magnitude study on signal flow graphs of semiconductor circuits to evaluate relative sensitivity of each circuit to values of individual circuit elements. For fluidic systems similar "brute force" approaches would yield indications of: 1) pressure response, 2) flow rate response, 3) relative pressure levels and 4) relative time constants. But such an approach may not be cost effective.

Boyle et al (reference 14) in discussing macromodels of large-scale integrated circuits point out that computational costs may preclude the

use of the most complex semiconductor circuit models in system simulation. They suggest that less comprehensive computational circuit models may produce highly inaccurate, if not invalid results.

Three major conclusions may be drawn from the above studies:

1. there is a need for evaluating circuit models in the context of physically realistic terminal conditions,
2. there is a need for devising meaningful steady state and dynamic error criteria which reflect cost, and
3. there is a trade-off between model accuracy in any given application and system simulation costs.

A model evaluation algorithm may be envisioned in which both a qualitative and a quantitative assessment is made of the relative quality of a particular fluidic circuit model.

The following ten step approach may be used for selecting a "best" equivalent circuit model for a physical fluidic component in a selected application. The definition of "best" depends on the tradeoffs between cost, accuracy, and other factors unique to the application. The judgment and experience of the designer ultimately will determine the criteria for "best".

1. Select a physical component within a physical system with realistic or typical terminal load conditions (established by other physical components) which do not "mask" the basic character of response of physical processes of that physical component.
2. Identify the basic physical processes within the entire physical system including the physical component of interest.
3. Collect or formulate one or more component (circuit) models

(topological structures and element parameters) of the physical component and connected physical terminal components in the physical system. The set of component models should include one model which is suitable as a reference for each component.

4. Validate the reference model over the operating range of interest using experimental evidence from the literature or a critical experiment on the physical component with typical physical terminal components.
5. Compute steady state and dynamic response for each component model with loading conditions typical of those in the selected system. For example, compute phase plane trajectories ($\dot{p}$ versus p) based on a pressure step input or compute Bode plots ($|P(s)/P_{ref}(s)|$) and arctan ($P(s)/P_{ref}(s)$)) based on a small signal sinusoidal input.
6. Define error criteria for comparing a particular circuit model of the physical component with the reference model.
7. Compute steady state and dynamic errors between each model and the reference model from the simulated responses.
8. Define a "cost" or "penalty" factor which is a measure of the relative complexity of and cost of simulating each circuit model within a large network.
9. Compute and compare penalized steady state and dynamic errors between each model and the reference model.
10. Select a "best" model of the given physical component (with given load conditions) based on the penalized error in step 9.

The key question is, which one of the several circuit models available should be used in the analytical design of a system using the component? Cost, time, and availability of suitable test equipment may prevent or inhibit the execution of step 4. The systems analyst can still select a reference model which he believes to be of sufficient accuracy for the particular application. Model evaluation based on this reference model will yield information concerning the relative accuracy and cost associated with using a particular model in a systems design application.

Considerations and procedures related to the above ten steps are discussed below.

Identification of Basic Physical Processes

The fluidic components chosen for study in this thesis are among the most important of all the passive elements; i.e., capillary modules, enclosed volumes, and bellows modules. Three basic physical processes are apparent in the study of these real components: 1) energy dissipation,[1] 2) energy storage in the form of potential energy, and 3) energy storage in the form of kinetic energy.

A fluidic resistance is commonly represented (reference 12) by a steady-state constitutive relationship (Figure 1) between volume flow

---

[1]The term "energy dissipation" is used by Shearer et al. (reference 12) as a general descriptor which applies to power loss ($P_{21} \times Q$) due to head losses. A rigorous thermodynamic definition is not implied by "energy dissipation" because only a portion of the "dissipated energy" is unrecoverable -- much is available in the form on internal energy.

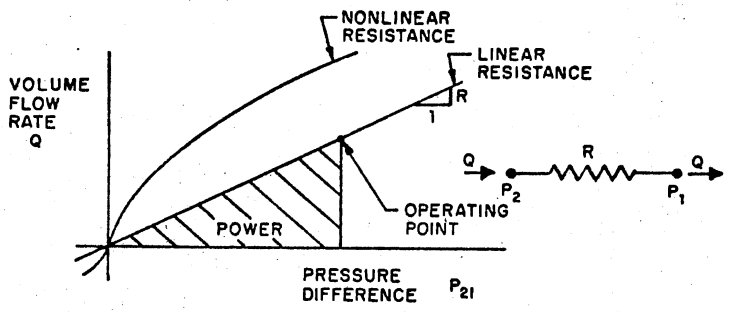

Figure 1. Constitutive Relationship for Fluidic Resistance

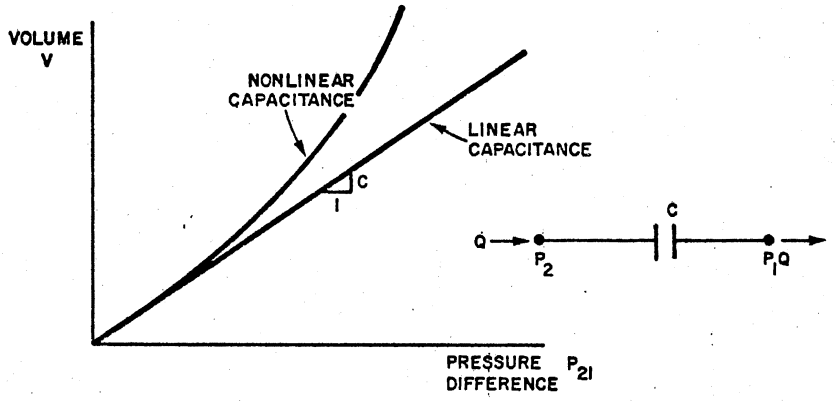

Figure 2. Constitutive Relationship for Fluidic Capacitance

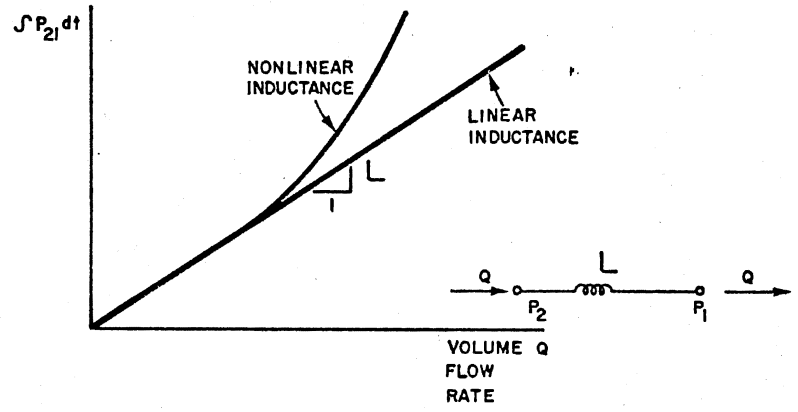

Figure 3. Constitutive Relationship for Fluidic Inductance

rate, Q, and pressure drop, P_{21},[2] as follows

$$Q = f(P_{21}) \tag{2.1a}$$

and

$$\text{sign } (Q) = \text{sign } (P_{21}) \tag{2.1b}$$

where Q = 0 when $P_{21} = 0$. The power dissipated by the resistance element is the product of volume flow rate, Q, and pressure difference, P_{21}, between the two external terminals (schematically shown as the area under the Q (P_{21}) curve from the origin to the operating point in Figure 1.

$$\text{Power} = P_{21} \times Q(P_{21}) \tag{2.1c}$$

Fluidic energy dissipation results from viscous shear in fully developed flow and transfer of momentum between layers in developing flow. While the latter is typically nonlinear energy dissipation, the former may be either nonlinear or linear energy dissipation (Figure 1).

Energy may be stored as potential energy either as a result of compressibility of the fluid or as a result of the volume change due to the mechanical deflection of a moveable member adjacent to the fluid. In either case, the volume of fluid changes. Both storage mechanisms are represented (reference 12) by a constitutive relationship (Figure 2) between instantaneous volume of the fluid, V, and instantaneous pressure drop, P_{21}, as follows:

$$V \equiv \int Q \, dt = f\ (P_{21}) \tag{2.2}$$

where the volume of fluid, V, is the time integral of the volume flow

---

[2] It is assumed throughout this thesis that pressure differences are small compared to average pressures. It is appropriate then to use volumetric rate of flow, Q, as the through variable for both liquid and gaseous fluids. Pressure drop, P_{21}, is the across variable, the pressure drop between P_2 and P_1.

rate, Q. The two curves in Figure 2 represent linear and nonlinear potential energy storage, respectively.

Also, energy may be stored as kinetic energy when the moving fluid accelerates as a result of forces on it. A constitutive relationship which describes this energy storage effect is

$$\int P_{21}\, dt = f(Q) \qquad (2.3)$$

The two curves in Figure 3 represent linear and nonlinear kinetic energy storage, respectively.

Circuit Model Formulation

A fluidic system is composed of components that supply energy as well as of the components that dissipate and store energy. A component that supplies energy is an active component; a component that receives energy (with subsequent dissipation or storage) is a passive component. Models of fluidic components are considered distributed when represented by partial differential equations and are considered lumped when represented by ordinary differential equations. When the temporal changes within the processes dominate over the spatial changes, the lumped parameter approach is generally adequate.

A component or a process within the component which exhibits mainly energy dissipation or mainly energy storage is most simply represented by a lumped parameter model. A lumped parameter element, which has two external terminals at which energy is interchanged with the environment, is termed a two-terminal or a one-port element. A "pure" element exhibits only one energy process. Three pure lumped parameter elements may be identified (reference 12):

1. A fluidic resistor, which dissipates energy has a resistance,

R, defined as follows:

$$R = \frac{f(P_{21})}{Q} \tag{2.4}$$

The incremental slope of the curve of Q versus P_{21} is the resistance, R (Figure 1). A linear resistor has a constant value of R.

2. A fluidic capacitor, which stores energy in the form of potential energy, has a capacitance, C, defined as follows:

$$C = \frac{\int Q\, dt}{f(P_{21})} \tag{2.5}$$

Capacitance is therefore the incremental slope of the curve of V versus P_{21} (Figure 2). A linear capacitor has a constant value of C.

3. A fluidic inductor, which stores energy in the form of kinetic energy, has an inductance, L, defined as follows:

$$L = \frac{f(Q)}{\int P_{21}\, dt} \tag{2.6}$$

The incremental slope of the curve of $\int P_{21}\, dt$ versus Q (Figure 3) is the inductance, L. A linear inductor has a constant value of L.

Depending upon the energy processes occuring in the individual fluidic component, the lumped-parameter circuit model may take the form of just one or an array of the above basic or "pure" circuit elements. The parameters of these circuit elements -- R, L, and C -- may be constants, functions of the pressure or functions or frequency or both.

Distributed parameter models must be considered if high signal frequencies occur in physical components such as capillary modules. Such components may be modeled as transmission lines. Although the

same energy processes -- dissipation and storage -- occur, they may be combined in different ways (reference 17). A method of characteristics approach including fricitional effects is one technique which may be applied to compute the response of a distributed parameter model.

Circuit Model Simulation

Lumped passive circuit elements (reference 18) may be interconnected to form a topological array or a set of closed paths. Each circuit element is connected to one or more other circuit elements at two or more circuit nodes. A branch is a section of a circuit between circuit nodes. Two or more circuit elements are connected at each node. A loop is a closed path which starts at a node, passes through two or more different branches and one or more different nodes, and ends at the original node.

The algebraic and integral equations for the basic circuit elements (equations 2.4, 2.5, and 2.6) are branch equations. Each fluidic loop equation may be interpreted as a mathematical description of the physical principle of conservation of energy. A loop equation for a fluidic circuit is the sum of potential drops (static pressure drops) around the loop. Each node equation may be interpreted as a mathematical relationship that describes the physical principle of mass conservation. For incompressible flow, the fluidic node equation describes conservation of volume flow, Q, at each node.

Branch, loop, and node equations for a lumped parameter model of a given circuit topology are generally solved by three standard forms of circuit analysis (reference 19) -- branch, loop, or node analysis.

Experimental Validation of Reference Model

Validation of a reference model is best accomplished through the use of steady state and dynamic response measurements on the real physical component. Experimental test apparatus and procedures utilized by the author in validating reference models are described below.

Due to difficulties of interpreting frequency response plots for nonlinear processes, a choice was made in these studies to evaluate dynamic circuit models of passive fluidic components in the time domain.

The transient response measurement apparatus shown in Figure 4 includes a pressure step function generator and a pair of pressure signal transducers with measuring and recording devices. Rise time and duration of the pressure step signal must be considered with respect to time constants of physical components being tested. When the shortest time constants are in the order of 10 msec, a fast rising pressure step (< 1 msec) is produced by a fast-acting solenoid valve; the wave front is steepened in a transmission line about 6 m (20 ft) in length. The flat portion of the pressure step lasts about 30 msec before the first reflection changes the pressure level. Pressure steps up to about 25 kPa (3.7 psi) are possible with this apparatus when the line pressure is about 500 kPa (75 psi).

When the physical component time constants are substantially greater than 10 msec, the solenoid valve is connected directly to the physical component on test. Rise times to the final steady state pressure level are of the order of 5 msec. Step pressure levels as high as line pressure are available.

Kistler pressure transducer systems are used to measure instantaneous pressures for short time-constant components. Barocel pressure

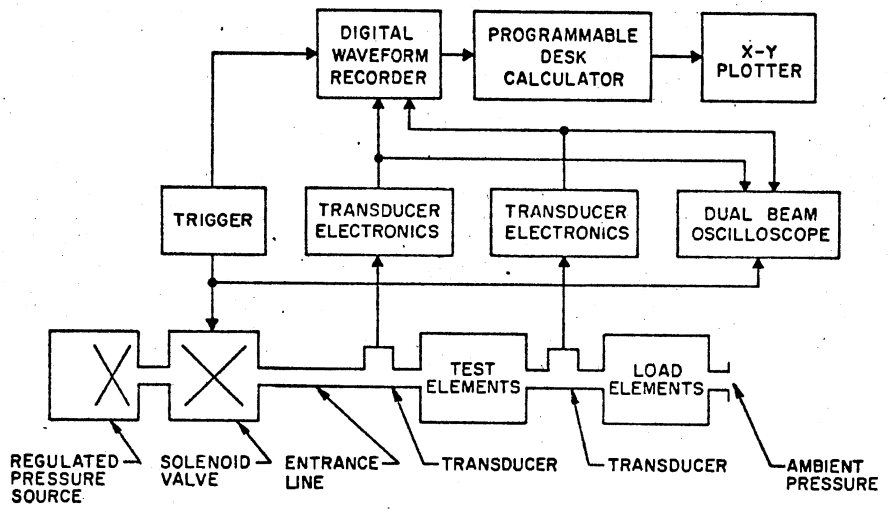

Figure 4. Schematic Diagram of Test Apparatus for Measuring Response of a Fluidic Component

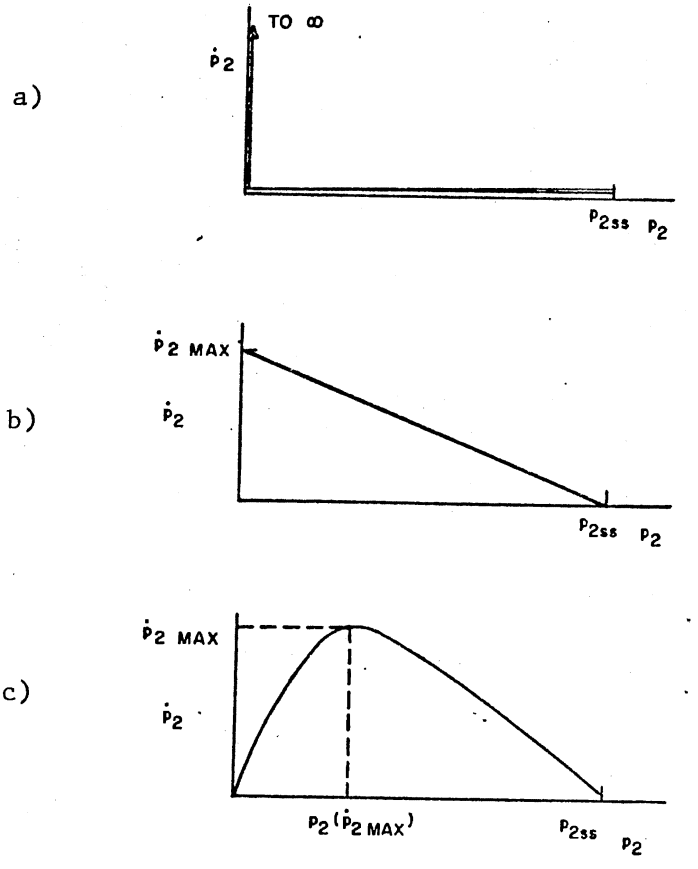

Figure 5. Typical Trajectories for Phase Plane Response

transducer systems are used to measure instantaneous pressures for long time constant components.

Pressure versus time traces are displayed on a dual beam oscilloscope as well as stored digitally in a Biomation 1015 waveform recorder. Data in the waveform recorder can then be recalled and digitally processed in a Wang 2200 programmable desk calculator (20 K memory).

Phase-Plane Trajectories

Transient pressure signals are readily displayed as pressure versus time traces. During the interesting initial transient pressure response of a dynamic system, the instantaneous slope of the trace changes radically. It was felt that in preliminary simulations of sets of component models, that pressure signatures were less sensitive to changes in circuit topology and element values than were the time rate of change (instantaneous slope) of the pressure signatures.

These observations suggested plotting transient response of dynamic system models as phase-plane trajectories. A phase-plane trajectory is a plot of pressure rate, $\dot{p}$, versus pressure, p. Here the phase-plane trajectory is a plot of pressure response rate, $\dot{p}_2$, versus pressure response, p_2, in response to a pressure step, $p_1(t)$.

The response of a set of component models produces a set of trajectories in the phase-plane. Although variations and trends are readily observed as models are changed, there is no sufficiently rigorous analytical means at present for selecting component models to shape phase-plane trajectories. The two points on the phase-plane trajectory of the major interest are felt to be the steady state end point ($\dot{p} = 0$, $p = p_{ss}$) and the pressure rate maximum ($\dot{p} = \dot{p}_{max}$,

$p = p(\dot{p} = \dot{p}_{max})$). Some interesting analytical results are noted by applying step pressure signals to generalized linear zeroth, first, and second order components.

Consider the response of a zeroth order model

$$p_2 = \alpha p_1 \tag{2.7}$$

Its phase plane trajectory is shown in Figure 5a initially to have zero rise time or infinite slope ($\dot{p}_2 = \infty$) and proceed instantaneously to the end point ($\dot{p}_2 = 0$, $p_2 = p_{2ss}$) so that from equation (2.7)

$$p_{2ss} = \alpha p_1 \tag{2.8}$$

For a first order model where

$$\dot{p}_2 + \beta p_2 = \alpha p_1 \tag{2.9}$$

the maximum value of $\dot{p}_2$ occurs initially (t = 0) (Figure 5b),

$$\dot{p}_{2max} = \alpha p_1 \tag{2.10a}$$

From equation (2.9) the steady state value is

$$p_{2ss} = \frac{\alpha}{\beta} p_1 \tag{2.10b}$$

so that

$$\dot{p}_{2max} = \beta p_{2ss} \tag{2.10c}$$

where β is the reciprocal of the time constant, τ, so that

$$\dot{p}_{2max} = \frac{p_{2ss}}{\tau} \tag{2.10d}$$

Therefore the maximum value of $\dot{p}_2$ for the step response of a first order system is inversely proportional to the time constant of the system and directly proportional to the steady state value.

In a second order system

$$\ddot{p}_2 + \gamma \dot{p}_2 + \beta p_2 = \alpha p_1 \tag{2.11}$$

a typical phase plane trajectory is shown in Figure 5c. Here

$$\dot{p}_{2max} = \frac{\alpha p_1 - \beta p_2(\dot{p}_{2max})}{\gamma} - \tag{2.12a}$$

From equation (2.11), the steady state value is

$$P_{2ss} = \frac{\alpha}{\beta} p_1 \tag{2.12b}$$

so that

$$\dot{p}_{2max} = \frac{\beta}{\gamma} p_{2ss} \left(1 - \frac{p_2(\dot{p}_{2max})}{p_{2ss}}\right) \tag{2.12c}$$

Since in equation (2.11) $\beta = \omega_n^2$, where ω_n is the undamped natural frequency of the second order system and $\gamma = 2\zeta\omega_n$, where ζ is the damping ratio; then

$$\dot{p}_{2max} = \frac{\omega_{n\ ss}}{2_\zeta} \left(1 - \frac{p_2\ (\dot{p}_{2max})}{p_{2ss}}\right) \tag{2.12d}$$

Therefore the point of the maximum pressure rate for the pressure step response of a second order system is a function of natural frequency and damping ratio.

Experimental phase plane plots are processed and plotted by the Wang 2200 from data acquired by the Biomation 1015 waveform recorder.

Penalty Factors

An array of ad hoc penalty factors (Table I) is selected on the basis of judgment and experience to quantitatively rank model complexity and computer simulation costs.

A zeroth order, lumped linear frequency independent circuit model (comprising component models of the test and load components) is assessed a multiplicative penalty factor of "1". Each order of the lumped circuit model adds an additional "1" to the penalty factor. For a total of N circuit elements, n of which are nonlinear and f of which

TABLE I

PENALTY FACTORS FOR COMPONENT MODELS

	Order of Terminated Component Model	Linear Frequency Independent Circuit	Nonlinear Frequency Independent Circuit with n Nonlinear R,L,C Elements (or Segments)	Linear Frequency Dependent Circuit with f Frequency Dependent L,C, Elements (or Segments)	Nonlinear Frequency Dependent Circuit with n Nonlinear R,L,C and f Frequency Dependent L,C Elements (or Segments)
Lumped Parameter Models with N Components	0	1	$1 + \frac{n}{N}$	$1 + \frac{f}{N}$	$1 + \frac{n+f}{N}$
	1	2	$2 + \frac{n}{N}$	$2 + \frac{f}{N}$	$2 + \frac{n+f}{N}$
	2	3	$3 + \frac{n}{N}$	$3 + \frac{f}{N}$	$3 + \frac{n+f}{N}$
Distributed Parameter Models (Method of Characteristic Solution) with s Intermediate Nodes	∞	$1 + \frac{s}{10}$	$1 + \frac{s}{10} + \frac{n}{s}$	$1 + \frac{s}{10} + \frac{f}{s}$	$1 + \frac{s}{10} + \frac{n+f}{s}$

N = number of circuit elements in lumped circuit model.
n = number of circuit elements described by nonlinear parameters.
f = number of circuit elements described by frequency dependent parameters.
s = number of segments in method of characteristics solution.

are described by frequency dependent parameters, the non-ideal description of the circuit elements adds a quantity $\frac{"n + f"}{N}$ to the penalty factor.

A distributed parameter model with a method of characteristics solution is assessed a multiplicative penalty factor based on the number of segments s into which the solution is divided. The penalty factor based on solution segments is $"1 + \frac{s}{10}"$. In a similar vein to the case of lumped circuit models, a quantity $\frac{"n + f"}{s}$ is added to penalty factors for distributed models.

Static and Dynamic Errors in the Phase Plane

Static and dynamic errors may be defined in terms of the computed phase-plane plots for the reference model (r) and the phase-plane plots for the models to be evaluated (m). The steady state error between the "(r)" and "(m)" models is defined as

$$E(p_{ss}) = \frac{p_{ss(r)} - p_{ss(m)}}{p_{ss(r)}} \tag{2.13a}$$

The dynamic error between the "(r)" and "(m)" models is defined as

$$E(\dot{p}_{max}) = \frac{\dot{p}_{max(r)} - \dot{p}_{max(m)}}{\dot{p}_{max(r)}} \tag{2.13b}$$

Penalized steady state and dynamic errors may be defined as products of the penalty factors (Table I) and the steady state and dynamic errors, i.e.,

Penalized steady state error $E(p_{ss})$ = Penalty factor x $E(p_{ss})$ (2.14a)

Penalized dynamic error $E(\dot{p}_{max})$ = Penalty factor x $E(\dot{p}_{max})$ (2.14b)

"Best" Model

"Best" model is defined as the one component model from a set of models which is calculated to be most adequate in the sense of having the least physical error as traded off against cost. The concept of "best" model is viewed in terms of a defined quantitative assessment (an evaluation algorithm) which is largely subjective. "Best" model refers to the relative quality of a set of models in terms of 1) model structure, 2) reference model structure, 3) physical terminations and their model structures, 4) signal level and bandwidth, and 5) error criteria. Three important questions, relative to completeness and adequacy of a set of models, are immediately called to mind.

1. Is the set of component models (including termination models) sufficiently complete?
2. Are the test conditions adequate to assess a "best" model? and
3. Are the error criteria adequate to assess a "best" model?

For the first question concerning completeness, at least one model from the set should be sensitive to the same amplitude range and bandwidth as the physical component under study. One or more models should correctly characterize the application for which the physical component is to be applied.

In regard to the second question on the adequacy of test conditions, it is important to recognize that a study of the component, which is "isolated" in the sense of defined termination (load) conditions, may lead to improper conclusions concerning the utility and validity of lumped-parameter models. That is, a lumped-parameter model of a fluidic network, having terminations with dominant dynamic elements, might be forced to operate at signal frequencies which would

either mask or erroneously intensify the signal frequencies of that lumped-parameter model of the test component. If a lumped parameter model is operated at a frequency on the order of the natural frequency of the lumped-parameter model, it is expected to perform poorly. For example, the calculated response of a lumped-parameter model to a step input (which contains all frequencies) would be expected to depart significantly from the response determined from experimental data. Even if a lumped-parameter model was subjected to a "step" input signal having a finite rise time (as in the case of a test input signal used to study validity of the evaluation algorithm), a significant discrepancy between measured and computed responses would likely still exist. It therefore seems reasonable that if the signal and frequency content of the test configuration can be established a priori, then the evaluation process for an "isolated" fluidic component can be carried out with a more suitable input signal.

In light of the third question on the adequacy of the error criteria for assessing a "best" model, both the non-penalized error and the penalized error always have a minimum value in progressing from a most simple to a most complex model (usually the reference model for a set of component models) in order for a valid assessment of a "best" model to be made. Cost does not enter into calculating non-penalized error, which is a function only of the selection of models, of a reference model, of imposed termination conditions, and of defined errors. However, penalty factors are selected and applied in order to reflect an added dimension of "cost". Penalized error, which is a meaningful assessment of both dynamic accuracy and cost, generally passes through a minimum in the vicinity of the "best model to indicate a simpler model than is indicated by a minimum value of non-penalized error.

CHAPTER III

FORMULATION AND EVALUATION OF CIRCUIT MODELS FOR A SELECTED SET OF FLUIDIC COMPONENTS

Approaches for the formulation and the evaluation (based on the algorithm discussed in Chapter II) of circuits models for two important passive components (a capillary module and an enclosed volume) that are commonly used in fluidic networks are briefly presented in this chapter. For completeness, circuit models for a bellows module are also presented (without applying the evaluation algorithm) in this chapter.

Circuit models for each of the three components are formulated in terms of one or more topological structures and one or more algebraic expressions valid over different operating ranges. Component models for the capillary module and for the enclosed volume are evaluated in the context of simple passive lumped-parameter circuits. A distributed parameter model of the capillary module is also discussed.

Capillary Module

The capillary module is a bundle of N identical right circular, parallel capillaries, each of radius r, and length, ℓ. Dissipation of energy in a circular capillary module is related to a nonlinear resistance, R_N, by the following expression (reference 3):

$$R_N = \frac{P_{21}}{Q} = \frac{8\mu\ell}{N\pi r^4} + \frac{7}{6}\frac{\rho}{N^2\pi^2 r^4}|Q| \qquad (3.1)$$

where μ is the absolute viscosity and ρ is the mass density of the fluid. The first term in equation (3.1) is the Poiseuille-law viscous shear loss (reference 2) for steady, fully-developed, laminar, incompressible flow. The second term in equation (3.1) is the loss due to transfer of momentum between layers in steady developing, laminar, incompressible flow.

Merritt (reference 4) indicates that in the laminar flow regime, the amount of error in using only the first term of equation (3.1) as the resistance of the capillary is less than 10 percent if the ratio of length to diameter, ℓ/d, is related to the Reynolds number, N_R, by the inequality.

$$\frac{\ell}{d} \geq 0.434\ N_R \tag{3.2}$$

Meritt maintains $\ell/d \geq 400$ to assure linearity within 10 percent.

When a time-varying pressure drop is applied across the capillary, compressibility and inertial phenomena produce dynamic effects. As a first-order dynamic correction, each capillary is assumed to be a short segment of a circular transmission line. In reference 5, the transmission line is modeled as a Poiseuille-law resistance, a constant linear capacitance, and a constant linear inductance (inertance). For a capillary module with N capillaries, the linear capacitance,[1] C_N, is given by:

$$C_N = \frac{N\pi r^2 \ell}{np_\infty} \tag{3.3}$$

where n is the polytropic coefficient, and p_∞ is the ambient absolute

---

[1]For small pressure variations, p_2', about the ambient pressure, p_∞, the static pressure, p_2, is given as $p_2 = p_\infty + p_2'$. A linear approximation is used to set $p_2 \approx p_\infty$.

static pressure. The linear inductance is given by:

$$L_N = \frac{\lambda \rho_\infty \ell}{N\pi r^2} \tag{3.4}$$

where ρ_∞ is the ambient mass density and from reference 5, λ is approximated as:

$$\lambda \doteq 1 + \frac{1}{3} \exp\left(-\frac{\omega r^2}{32\pi\nu}\right) \tag{3.5}$$

For sufficiently high frequencies that $\omega \geq \frac{100\ \nu}{r^2}$, then $\lambda = 1$.

For sufficiently low frequencies that $\omega \leq \frac{10\nu}{r^2}$, then $\lambda = 4/3$.

The ratio of linear inductive reactance, X_L, to linear resistance is determined from equations (3.4) and (3.1),

$$\frac{X_L}{R} = \frac{\lambda \omega r^2}{8\nu} \tag{3.6}$$

where ω is the radian frequency and ν is the kinematic viscosity. The ratio of linear capacitive reactance, X_C, to linear resistance is determined from equations (3.3) and (3.1),

$$\frac{X_C}{R} = \frac{n p_\infty r^2}{8\omega\mu\ell^2} \tag{3.7}$$

As the frequency increases, the inductive reactance increases and the capacitive reactance decreases relative to resistance.

For pressure variations which are not small compared to p_∞,

$$p_2 = p_\infty + p_2' \tag{3.8a}$$

and ρ_2 and p_2 are related through the process equation

$$\frac{\rho_2}{\rho_\infty} = \left(\frac{p_2}{p_\infty}\right)^{\frac{1}{n}}. \tag{3.8b}$$

Nonlinear capacitance (reference 20), C_N, and nonlinear inductance (reference 5), L_N, become

$$C_N = \frac{N\pi r^2 \ell}{np_\infty} \frac{1}{(1 + \frac{p_2'}{p_\infty})} \tag{3.9}$$

and

$$L_N = \frac{\lambda \rho_\infty \ell}{N\pi r^2} (1 + \frac{p_2'}{p_\infty})^{\frac{1}{n}} \tag{3.10}$$

With the expressions for R, L, and C above, it is possible to construct several equivalent circuits for a capillary module.

For steady flow through a capillary module, resistance alone describes the physical process and the equivalent circuit for this 0th order system is a resistor. The simplest 1st order system includes resistance and inertance effects as a series RL circuit. The simplest 2nd order system appends a grounded capacitor to the 1st order RL circuit. There are six possible topological structures for R, L, and C (suggested by reference 11). At low frequencies all perform similarly. At higher frequencies, where lumped parameter models are still acceptable but less adequate than distributed parameter models, differences in calculated frequency responses are reported in reference 21. The 0th and 1st order circuits are reduced topological structures of a 2nd order circuit with R, L, and C.

At high frequencies a capillary module is described as a distributed parameter (transmission line) model which is calculated herein by the method of characteristics using a digital computer program. The step response of a transmission line for finite amplitude signals, with no heat transfer but with wall shear losses is described in reference 17, pp 125-128. The storage processes (L, C) are entered implicitly through the initial value of acoustic velocity, a, and line length, ℓ. Dissipation is described in terms of the length, ℓ, as

well as the diameter, d, and a friction coefficient, $F = \frac{2f\ell}{d}$, where f is the classical friction factor.

Component models for the capillary module are evaluated below from the evaluation algorithm discussed in Chapter II.

Select Component and Termination or Load Components

A porcelain capillary module with 25 parallel right circular capillaries is selected. In evaluating its steady state and dynamic performance, terminations chosen for these tests are a) as the input terminal condition, a steady state input pressure and then a dynamic input pressure step with a finite rise time, and b) as the output terminal condition, an output capillary module which is terminated in the ambient plenum. Load capillary modules were selected to be approximately the same geometrically as the capillary module under study. This test configuration is shown in Figure 6. Generalization on the choice of a suitable load is impossible. However, it is reasonable to assume that the ultimate choice of the "best" model would not be strongly dependent on the choice of load. Therefore, the simplest and most typical situation to be encountered in the application is considered as the best choice.

The radius of each capillary passage is $r = 1.525 \times 10^{-4}$ m. Two lengths, $\ell = 0.1524$ m. (6.000 in.) and $\ell = 0.3048$ m. (12.000 in.) were used.

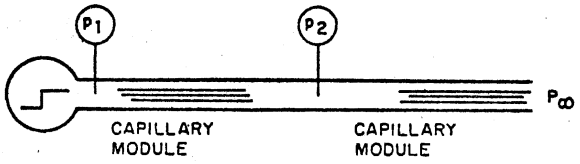

Figure 6. Test Configuration for Two Campillary Modules

a)

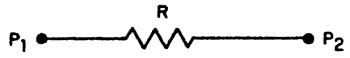

b)

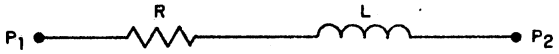

c)

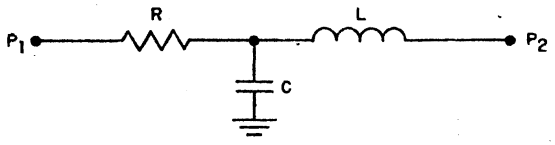

Figure 7. Simple Equivalent Circuit Models for Capillary

Identify Physical Processes of Component and Termination Components

In pneumatic systems both the capillary module of interest and the load capillary module display energy dissipation, energy storage through inertial accelerations, and energy storage through compressibility. For air at low frequencies the major energy process in a capillary is energy dissipation. For dimensions where $r/\ell << 1$, inertial storage processes predominate over compressibility storage processes. If static pressure is relatively constant, then each of these processes is essentially linear.

Collect or Formulate Component Models

A set of equivalent circuit models for the test and load capillary modules is selected from models presented above in this section. Linear and nonlinear, lumped-parameter, steady-state (0th order) and dynamic (1st and 2nd order) models are selected. The models chosen are as follows:

0th order (steady state) lumped model - capillary is modeled as a resistor (Figure 7a).

1st order (dynamic) lumped model - capillary is modeled as a resistor in series with an inductor (Figure 7b).

2nd order (dynamic) lumped model - capillary is modeled as a resistor and an inductor in series with a shunt to ground through a capacitor (Figure 7c). The second order RCL circuit model structure as shown in Figure 7c is the most complete one of this set.

Elements in the model are described as follows:

Resistor - linear resistor is described by the first term of equation (3.1) and the nonlinear resistor is described by both terms of equations (3.1).

Inductor - linear and nonlinear inductors are described by equations (3.4) and (3.10), respectively.

Capacitor - linear and nonlinear capacitors are given by equations (3.3) and (3.9), respectively.

In establishing a reference model for the capillary module, it is recalled (reference 11) that for small amplitude signals, a distributed parameter model is required if the line length, ℓ, is less than 0.1 wavelengths. At 1000 Hz the 0.1524 m. and the 0.3048 m. long capillary modules are 0.45 and 0.9 wavelengths, respectively. It is assumed arbitrarily that the reference model should be valid for signal frequencies of 500 Hz. In this case a distributed parameter model, rather than one of the above lumped parameter RCL models, is the best choice for the reference model.

A method of characteristics solution (reference 17) approach for large amplitude signals, neglecting heat transfer but including wall shear forces, was used to calculate the reference model response. For the distributed model, calculations were made in a method of characteristics solution. In this case a_∞ = 300 m/sec for air and a friction coefficient F = 300 to 500.

Experimentally Validate Reference Model

A total of six steady state and dynamic response tests were conducted with the capillary module with its load configuration.

Table II summarizes the parameters and test conditions used.

TABLE II

CAPILLARY RESPONSE TEST CONFIGURATIONS

	Test#	Test Capillary* Length	Load Capillary* Length	Input Signal Amplitude	Input Signal Rise Time
Static Tests	1	.1524m	.3048m	0-25 kPa	--
	2	.3048m	.3048m	0-25 kPa	--
Dynamic Tests	3	.1524m	.3048m	25 kPa	.001 sec
	4	.3048m	.3048m	25 kPa	.001 sec
	5	.1524m	.3048m	12.5 kPa	.001 sec
	6	.3048m	.3048m	12.5 kPa	.001 sec

*Radius = 1.525×10^{-4}m, N = 25.

Steady state output versus input pressure response (tests 1 and 2) were measured with Barocel strain gauge pressure tranducers. Results are plotted in Figure 8.

Time traces for dynamic tests 3 and 4 are shown in Figures 9a and 9b respectively. These data are replotted as the dotted curves on the phase-plane plots (Figures 10a and 10b). Pressure, p_2, was measured with a Kistler pressure transducer. The pressure, $\dot{p}_2$, was calculated from the p_2 versus time data using a 5-point numerical derivative.

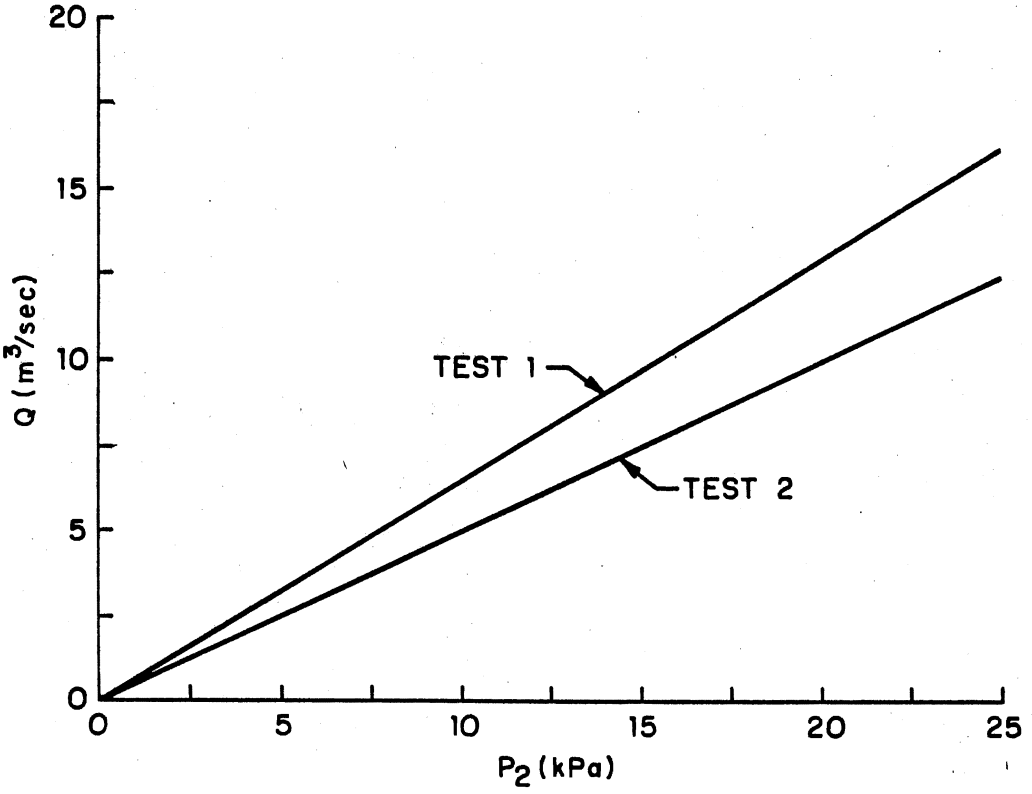

Figure 8. Steady-State Response for Two Series-Connected Capillary Modules

a)

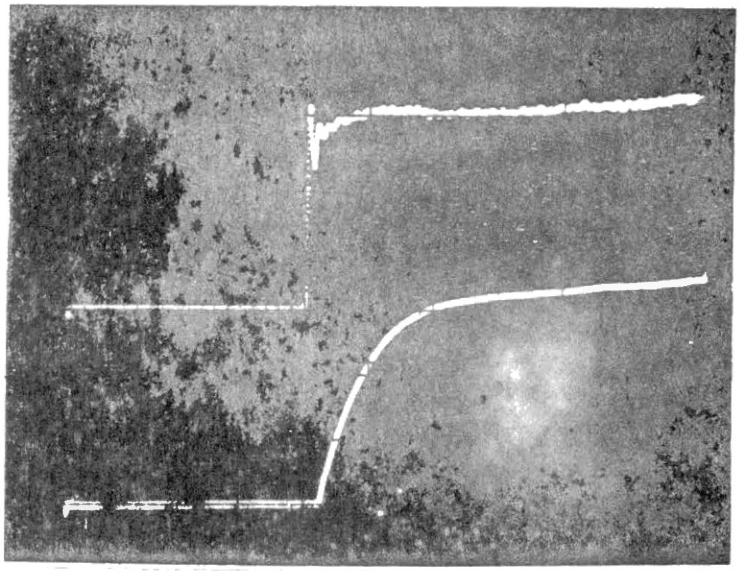

ℓ_1 = 0.154m, ℓ_2 = 0.3048m

b)

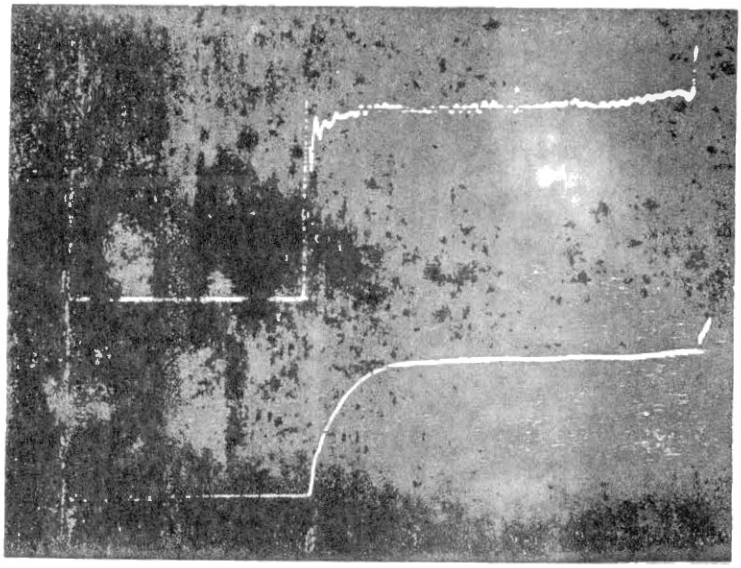

ℓ_1 = 0.3048m, ℓ_2 = 0.3048m

Figure 9. Time Traces From Dynamic Response Measurement on Two Series-Connected Capillary Modules

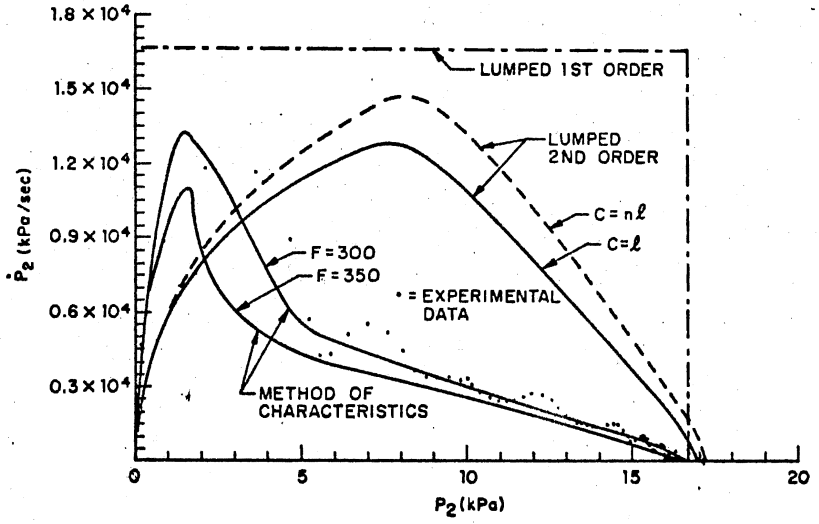

10a. Phase Plane Plots of Output Response for Test Capillary with Load Capillary (ℓ = .1525, .3048), $p_{1(max)}$ = 25 kPa

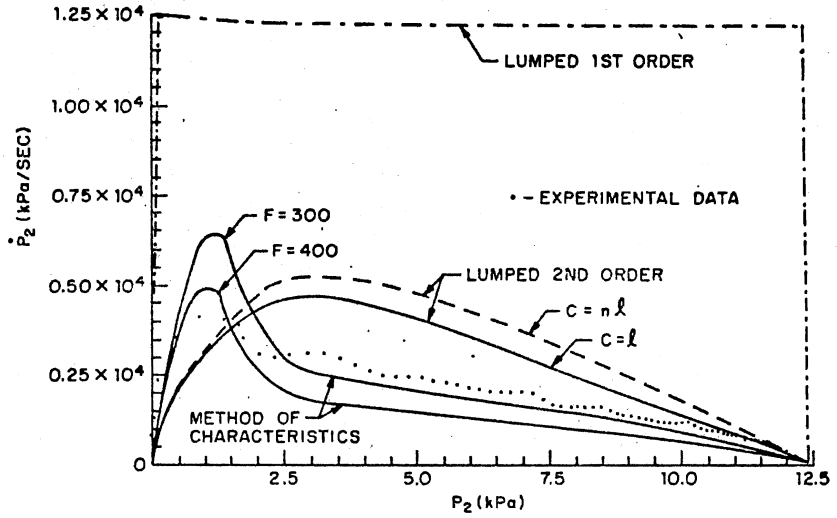

10b. Phase Plane Plots of Output Response for Test Capillary with Load Capillary (ℓ = .3048, .3048), $p_{1(max)}$ = 25 kPa

Compute Steady State and Dynamic Response

The response of several component models of the capillary with selected termination conditions was calculated. For the lumped first and second order models FNOL-2 (reference 22, a general program for solving simultaneous ordinary first order equations) was used. A BASIC version was run. Integration is performed in FNOL-2 with a variable step Adams-Moulton routine. A graphical output on an X-Y recorder could be selected. A finite rise time step input equivalent to that obtained with experimental apparatus was used for all step response calculations. No zeroth order responses were computed independently; the final steady-state values of the first and second order simulations were used instead.

The most complete lumped equivalent circuit model (Figure 11) of the test configuration comprises a second order equivalent circuit model for both the test and the load capillary modules. The selected second order RCL capillary model is composed of three components R_1, C_1, and L_1. The input termination (node p_1) is driven by a step pressure generator with a rise time, τ_{in}. The output termination (node p_2) is also a second order RCL capillary model (R_2,C_2,L_2), which is itself terminated at ground. This highest order general circuit is implemented with a set of loop equations which are defined by four state equations (3.11a,b,c,d) in terms of four state variables, y_1,y_2,y_3, and y_4.

$$\dot{y}_1 = \frac{d}{dt}\left[\int_o^t Q_1\, dt\right] = \frac{p_1}{R_1} - \frac{1}{L_1C_1}\, y_1 - \frac{1}{L_1}\,(y_3 + y_4) \qquad (3.11a)$$

$$\dot{y}_2 = \frac{d}{dt}\left[\int_o^t Q_2\, dt\right] = -\left(\frac{1}{L_1} + \frac{1}{L_2}\right) y_3 - \frac{1}{L_1}\, y_4 \qquad (3.11b)$$

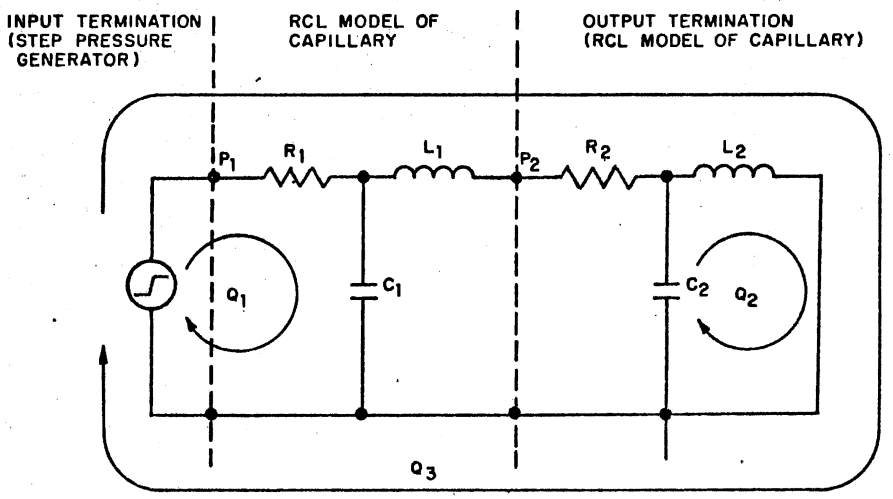

Figure 11. Circuit Diagram for Second Order RCL Model of Capillary With Terminations

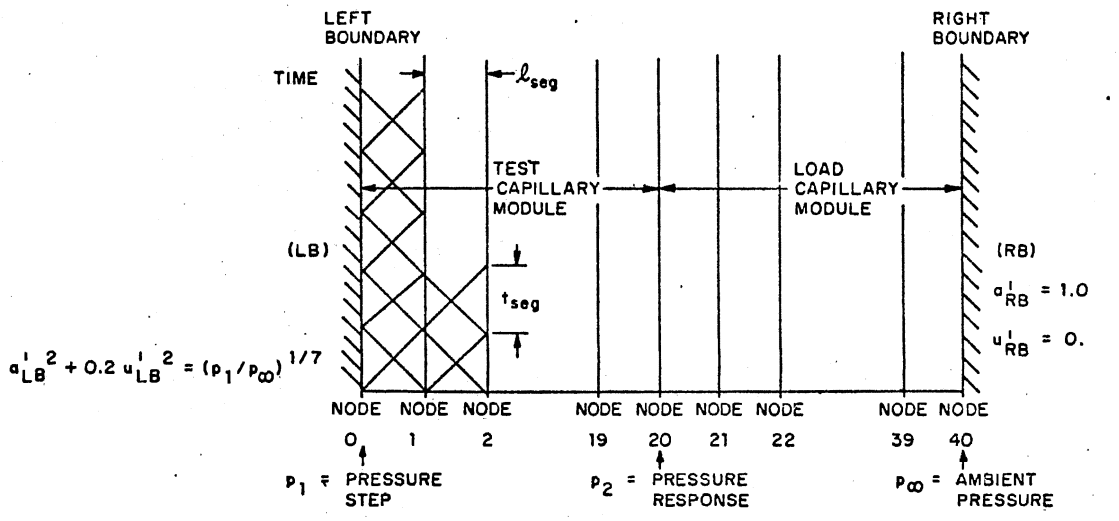

Figure 12. Position-Time Diagram for Method of Characteristics (Test 4)

$$\dot{y}_3 = \frac{y_2}{C_2} \tag{3.11c}$$

$$\dot{y}_4 = \frac{y_1}{C_1} - \frac{R_1}{L_1}(y_3 + y_4) \tag{3.11d}$$

with initial conditions

$$y_1 = 0 \tag{3.12a}$$

$$y_2 = 0 \tag{3.12b}$$

$$y_3 = 0 \tag{3.12c}$$

$$y_4 = 0 \tag{3.12d}$$

The four linear and nonlinear first order differential equations for this lumped model are solved with the FNOL-2 program. This set of equations, where the R_i, C_i, L_i are specified in step 3 above, is input into the FNOL-2 program. From the solution of the loop equations (3.11), p_2 is given as

$$p_2 = \frac{R_2}{L_1}(y_3 + y_4) - \frac{y_2}{C_2} \tag{3.13a}$$

but $\dot{p}_2$ must be evaluated numerically, from

$$\dot{p}_2 = \frac{R_2}{L_1}(\dot{y}_3 + \dot{y}_4) - \frac{\dot{y}_2}{C_2} + \frac{(R_2 - R_2')}{(L_1 - L_1')(t - t')}(y_3 + y_4) - \frac{(C_2 - C_2')}{(t - t')}\frac{y_2}{C_2} \tag{3.13b}$$

where R_2', L_1', C_2' are values of R_2, L_1, and C_2, respectively calculated at a previous value of time, t'.

A phase-plane plot ($\dot{p}_2$ vs p_2) is a graphical output of FNOL-2. Results of simulations for several combinations of linear and nonlinear (lumped) circuit models are presented in the phase-plane plots of Figures 10a and 10b.

The method of characteristics solution technique (reference 17) was however used to determine the step response for the reference model. Figure 12 demonstrates the wave diagram format corresponding to test 4. A FORTRAN program (pp. 469-471 in reference 17) was modified to compute the wave diagram solution. A wave diagram may be conceptualized where linear position is in the horizonal direction and time is in the vertical direction. Both test and load capillaries are divided into segments of length 0.01524 m (20 segments per foot). For the two demonstrated cases, the pair of 0.3048 m capillaries are discussed as one long 0.6096 m capillary (40 segments) in which p_2 is evaluated at node 20, between the 20th and 21st computational segments. Similarly the 0.1524 m and 0.3048 m capillaries are considered as one long 0.4572 m capillary (30 segments). Time is divided into intervals, t_{seg}, equal to the propagation time of a signal travelling across the length, ℓ_{seg}, of one spatial segment at acoustic velocity, a_∞

$$t_{seg} = \frac{\ell_{seg}}{a_\infty} \tag{3.14}$$

In reference 17 as well as in this discussion, velocity is normalized with respect to the acoustic velocity (a_∞ = 330 m/sec), length with respect to a characteristic length (total propagation length) for the pair of capillaries: ℓ = 0.6096 m or 0.4572 m), and time with respect to a characteristic time ($t_{char} = \ell_{char}/a_\infty$).

The normalized boundary conditions for a pressure step at the left boundary (LB) are given by equation (3.143, reference 17) and below as

equation (3.14)

$$a'^{2}_{LB} + 0.2\, u'^{2}_{LB} = \left(\frac{P_1}{P_\infty}\right)^{1/7} \tag{3.15a}$$

where a' and u' are normalized acoustic and particle velocities respectively. At the right boundary (RB), an ambient plenum is described for a method of characteristics solution as

$$a'_{RB} = 1.0 \tag{3.15b}$$

$$u'_{RB} = 0. \tag{3.15c}$$

These right boundary conditions were introduced into the FORTRAN program (pp. 469-471, reference 17). The method of characteristics solutions for the reference models in tests 3 and 4 are also plotted on Figures 10a and 10b.

Define Error Criteria

The steady state and dynamic error criteria are given by equations (2.13a) and (2.13b) in Chapter II.

Compute Steady-State and Dynamic Errors

The steady-state error, as defined by equation (2.13a) was negligible in Figures 10a and 10b. Dynamic errors were computed from Figures 10a and 10b, using equation (2.13b). Results are tabulated in Table III.

Define Penalty Factors

Penalty factors shown in Table I (Chapter II) were used to compute penalized dynamic errors.

TABLE III

COMPARISON OF ERRORS IN EVALUATION OF CAPILLARY MODELS

Capillary Model				Penalty Factor	Dynamic Error $E(\dot{p}_{2max})$	Penalized Dynamic Error
Order	R	L	C			
Capillary $r=1.525\times10^{-4}$ m N=25 Test Length$_1$=0.1524 m Test Length$_2$=0.3048 m P_1 = 25.0 kPa						
Lumped						
0	ℓ			1	1	1
0	$n\ell$			2	1	2
1	ℓ	ℓ		2	.27	.55
2	ℓ	ℓ	ℓ	3	.04	.13
2	ℓ	$n\ell$	ℓ	3.3	.02	.07
2	$n\ell$	ℓ	ℓ	3.3	.06	.22
2	ℓ	ℓ	$n\ell$	3.3	.10	.34
2	$n\ell$	$n\ell$	$n\ell$	4	.10	.39
Distributed						
∞	F = 350			5	.15	.74
∞	F = 300			Reference Model		
Capillary $r=1.525\times10^{-4}$ m N=25 Test Length$_1$=0.3048 m Test Length$_2$=0.3048 m P_1 = 25.0 kPa						
Lumped						
0	ℓ			1	1	1
0	$n\ell$			2	1	2
1	ℓ	ℓ		2	1.60	3.21
2	ℓ	ℓ	ℓ	3	.04	.13
2	ℓ	$n\ell$	ℓ	3.3	.02	.07
2	$n\ell$	ℓ	ℓ	3.3	.08	.28
2	ℓ	ℓ	$n\ell$	3.3	.08	.28
2	$n\ell$	$n\ell$	$n\ell$	4	.10	.42
Distributed						
∞	F = 350			5	.35	1.77
∞	F = 400			Reference Model		

Compute Penalized Steady State and Dynamic Errors

Penalized dynamic errors, computed from equations (2.13a) and (2.13b) are also tabulated in Table III.

Select a "Best" Model

As discussed in Chapter II, for both test cases 3 and 4, the computed penalized dynamic error in Table III passes through a minimum close to the "best" selected model. Use of the concept, "penalized error," permits a "best" model to be chosen with respect to a reference model. Here the "best" equivalent circuit model for the capillary within the test conditions and defined error and penalty criteria is a second order (RCL) model with linear resistance and capacitance and nonlinear inductance. Also it is apparent that the penalized error results lead to the same conclusion as the non-penalized error. That is, application of the penalty factors, chosen to reflect the added dimension of "cost", leads to the same conclusion as the simple error which reflects the dimension of dynamic "accuracy" only.

Enclosed Pneumatic Volume

A tank and a cavity with almost closed surfaces are fluidic structures that are classified as enclosed volumes. A rigid-walled enclosed volume stores energy by virtue of the fluid compressibility. The often used expression for the capacitance is

$$C = \frac{V}{np_{\infty}} , \qquad (3.16a)$$

where V is the volume of the capacitor, n is the polytropic exponent,

and p_∞ is the ambient pressure. A nonlinear model (reference 20) should be used if the static pressure, p_2, is unequal to p_∞. Here

$$C = \frac{V}{np_\infty}\left(1 + \frac{p_2'}{p_\infty}\right) \qquad (3.16b)$$

For both the linear and nonlinear models the equivalent circuit is a grounded capacitor (Figure 13a).

The simple definition for capacitance (equation 3.16a) fails to account for several factors:

(1) Changes in pressure, p_2', about steady state. -- The assumption of constant pressure restricts the model to small changes in pressure about the average.

(2) Thermodynamic processes. -- The thermodynamic process (discussed below) causes the polytropic coefficient, n, to be related to rate of change (frequency) of pressure (as well as to geometry). Under conditions that are partially isothermal and partially adiabatic, frequency-dependent volume compressibility as well as frequency-dependent energy dissipation are attributed to the thermodynamic processes in the volume.

(3) Geometry of the volume. -- The polytropic coefficient, n, is a function of the shape of the volume. (Katz and Hastie, reference 7, have considered n as a function of cylindrical, spherical and rectangular volumes.) In addition, the shape of the volume becomes important when the wavelength becomes comparable to the largest dimension of the volume. For short wavelengths (high frequencies), a lumped-parameter formulation for capacitance (equations 3.16) is not valid.

Katz and Hastie (reference 7) have investigated a cylindrical volume and shown that energy storage in fluid compressibility is given

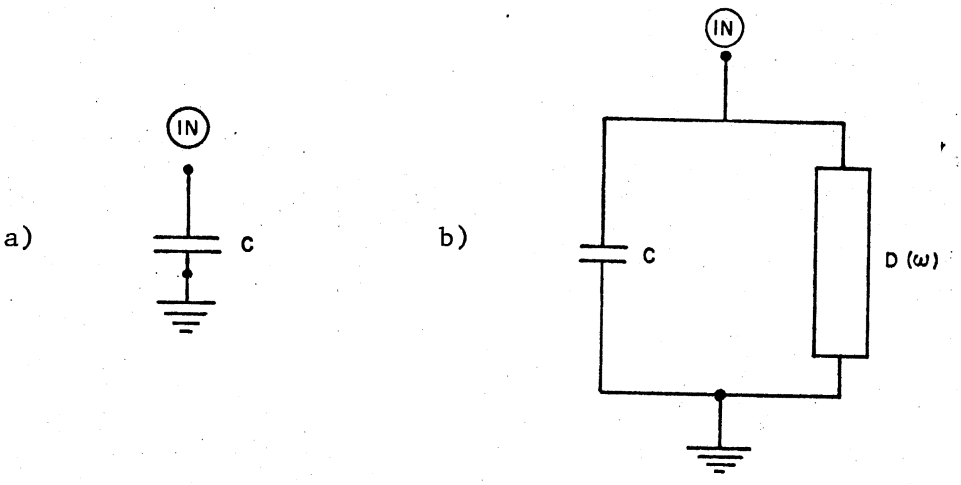

Figure 13. Equivalent Circuit Models of Tank (Enclosed Pneumatic Volume)

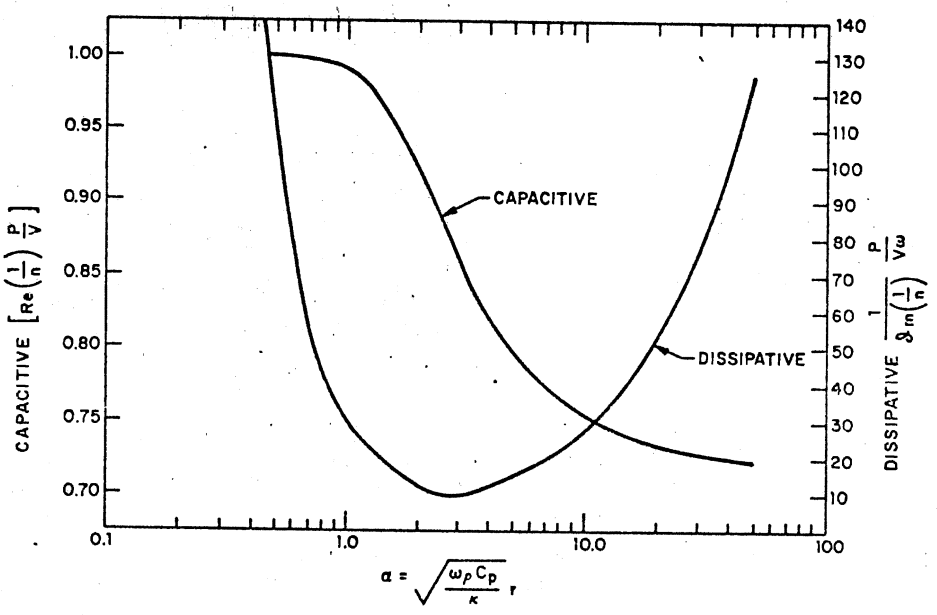

Figure 14. Frequency-Dependent Capacitance and Dissipation for Tank (Enclosed Cylindrical Volume)

by a frequency-dependent capacitance, $C(\omega)$, shunted to ground in parallel with a frequency-dependent dissipation $D(\omega)$, as shown in Figure 13b. Capacitance and dissipation are evaluated as

$$C(\omega) = \frac{V}{p_\infty} f_1(n) \tag{3.17a}$$

$$D(\omega) = \frac{P_\infty}{V\omega} f_2(n) \tag{3.17b}$$

where

$$f_1(n) = \left[\frac{1}{\gamma} - \frac{\gamma-1}{\gamma}\frac{\sqrt{2}}{\alpha}\frac{\mathrm{ber}_o\alpha\mathrm{ber}_1\alpha + \mathrm{bei}_o\alpha\mathrm{bei}_1\alpha - \mathrm{bei}_o\alpha\mathrm{bei}_1\alpha + \mathrm{ber}_1\alpha\mathrm{bei}_o\alpha}{\mathrm{ber}_o^2\,\alpha + \mathrm{bei}_o^2\alpha}\right] \tag{3.18a}$$

$$f_2(n) = \left[\frac{\gamma-1}{\gamma}\frac{\sqrt{2}}{\alpha}\frac{\mathrm{ber}_o\alpha\mathrm{ber}_1\alpha + \mathrm{bei}_o\alpha\mathrm{bei}_1\alpha + \mathrm{ber}_o\alpha\mathrm{bei}_1\,\alpha - \mathrm{ber}_1\alpha\mathrm{bei}_o\alpha}{\mathrm{ber}_o^2\,\alpha + \mathrm{bei}_o^2\,\alpha}\right]^{-1} \tag{3.18b}$$

$$\alpha = r\sqrt{\frac{\omega\rho C_p}{\kappa}}\,, \tag{3.18c}$$

where the ber and bei functions are Kelvin functions of zero and integer order, C_p is the specific heat at constant pressure, κ is the thermal conductivity, and γ is the ratio of specific heats.

In terms of the argument, α, it can be shown that

as $\alpha \to 0$,

$$C(\omega) = \frac{V}{P_\infty} f_1\,(n) \to \frac{V}{p_\infty}, \text{ the isothermal case;} \tag{3.19a}$$

as $\alpha \to \infty$,

$$C(\omega) = \frac{V}{p_\infty} f_1\,(n) \to \frac{V}{\gamma P_\infty}, \text{ the adiabatic case;} \tag{3.19b}$$

and as $\alpha \to 0$ and $\alpha \to \infty$,

$$D(\omega) = \frac{p_\infty}{V} f_2\,(n) \to \infty. \tag{3.19c}$$

When $D(\omega) \rightarrow \infty$, then $D(\omega)$ is essentially an open circuit and the a-c energy dissipation is essentially zero. Of course $D(\omega)$ is in shunt to ground and does not produce any series dissipation.

Capacitance and frequency-dependent energy dissipation for a cylindrical volume are plotted in Figure 14. Frequency dependent energy dissipation has a minimum value when the argument $\alpha = 3$. Below a value $\alpha = 0.52$ and above a value $\alpha = 40$, energy dissipation is at least an order of magnitude greater than that of its minimum value.

Capacitance is within one percent of its isothermal value for values of $\alpha < 1$ and within one percent of its adiabatic value for $\alpha > 50$.

Circuit models for the enclosed volume may be evaluated using the evaluation algorithm presented in Chapter II. The procedure is summarized below.

Select Component and Termination or Load Components

An aluminum cylindrical tank (Figure 15) with continuously adjustable height, h, was selected. As in the case of a capillary module, because generalization of a load was impossible, a simple and typically encountered application was selected for evaluating performance for essentially dynamic operation with through flow. In this evaluation procedure the tank is connected to two capillary modules as shown schematically in Figure 16 -- capillary module 1 driven by a pressure step signal (with finite rise time) and capillary module 2 terminated by the ambient plenum. The tank (Figure 15) is designed to accept as many as five connections. This component has an internal radius of

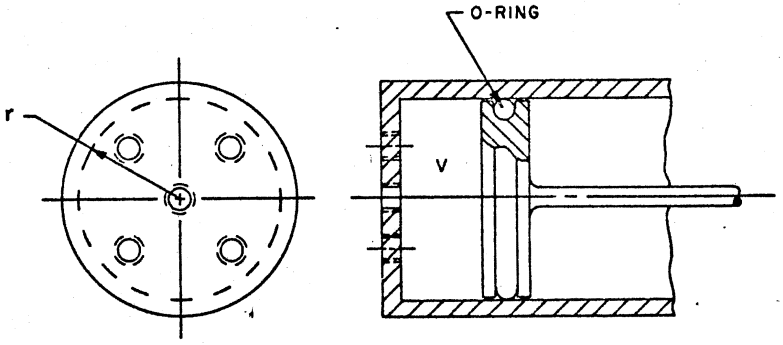

Figure 15. Pneumatic Tank

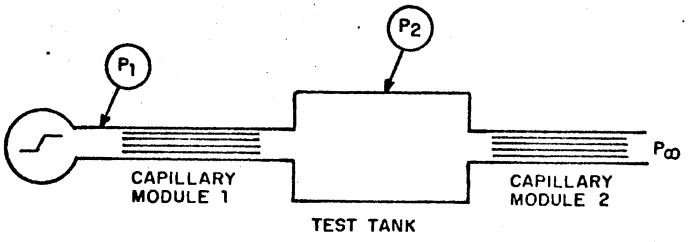

Figure 16. Test Configuration for Tank and Two Capillaries

$r = 2.54 \times 10^{-2}$ m (1.00 in), and a volume which is adjustable from 6.45×10^{-7} m^3 to 5.0×10^{-4} m^3. In these tests it is set at a height of h = 0.0210 m (0.827 in) or $V = 4.25^{-3} \times 10^{-3}$ m^3 (2.59 in^3). Capillary modules 1 and 2, which were evaluated above, are used here in evaluating the dynamics of this tank. Capillary modules 1 and 2 have 25 parallel passages, each of lengths ℓ = 0.3048 m and with radii $r = 1.525 \times 10^{-4}$ m.

Identify Physical Processes of Component and Termination Components

For the tank the major energy process is energy storage in gas compressibility. The polytropic coefficient, n, is frequency dependent, limited by the isothermal process at low frequencies (where n = 1.0) and the adiabatic process at high frequencies (where n = 1.4 for air). Depending upon the operating rate or frequency, the capillary modules dissipate energy and store kinetic or potential energy. In this example, the volume of the tank was so much larger than volume of the capillary modules that gas compressibility (capacitance) could be neglected with respect to capacitance of the tank. Further, for sufficiently slow charging rates for the tank, the inertance of the parallel capillary passages could be judged negligible with respect to the capacitive effects of the tank. If, for the physical processes in the tank and the capillary modules, the static pressure remains essentially ambient, then these processes are fundamentally linear.

Collect or Formulate Component Models

The set of equivalent circuit models for the test tank and the two

load capillary modules presented in the section above are used herein. A set of lumped-parameter, linear and nonlinear, dynamic (1st order) circuit models with the polytropic coefficient representing adiabatic, isothermal, or frequency-dependent processes are selected for the tank.

1st order (dynamic) model. Enclosed volume (tank) is modeled as a capacitor.

Capacitor. Is a function of the polytropic coefficient n = 1.4, 1.0, or $1/f_1(n)$ (from equation (3.18a)) for adiabatic, isothermal, or frequency-dependent processes, respectively. Linear and nonlinear capacitors are given in equations (3.16a) and (3.16b) respectively.

With the same 0th, 1st and 2nd order lumped-parameter (equivalent circuit) component models for the two capillary modules (presented above) various system models are defined.

In one test range of interest, the average pressure in the tank remains at nearly ambient pressure while the process can vary from high frequencies initially to d-c (as in charging a tank). Thus a linear, frequency-dependent circuit model is selected as the reference model in the evaluation. The reference model for the capillary modules with the signal frequencies developed from an input step signal in this component array is assumed to be a second order lumped-parameter equivalent circuit model.

Katz, in finding transient response for a frequency-dependent tank (reference 17), which is represented analytically in the s-plane, assumes an input pressure step through a linear resistor into a tank (a blocked load). The same technique can be applied for through flow in this configuration for a pressure step into a linear capillary, through a tank, and out through a linear capillary. Katz's equations (2.70) and (2.71a)

from reference 17 for transient pressure response of the tank apply directly to this test case if Katz's time constant, τ_a, is modified in the problem (for a linear input resistor, R_1, and a linear output resistor, R_2).

$$\tau_a = (R_1 + R_2) \frac{V}{\gamma p_\infty} \tag{3.20}$$

Experimentally Validate Reference Model

The test configuration consists of a (dynamic) pressure-step source, a tank, and two capillary modules as input and output loads (Figure 16). The same capillary modules were employed in this validation as in the capillary model evaluation process. They have 25 capillary passages which are 0.1524 m and 0.3048 m long with radii of 1.524×10^{-4}m. For this tank, radius r = 0.0254 m and volume $V = 4.24 \times 10^{-5}$ m^3. Input pressure steps of p_1 = 25 kPa with rise times of 50 msec and 5 msec were used to drive the circuit.

Experimental step response data were processed with the Biomation/Wang system and plotted to give the dotted curve plots on Figure 17. Pressure, p_2, was measured with a Kistler transducer system. Again pressure rate is calculated by a BASIC program using a five point derivative formula.

Compute Steady State and Dynamic Response

With the exception of the frequency dependent models, all transient circuit simulations were run with a BASIC version of FNOL-2. The most complete equivalent circuit model for the loaded test configuration (Figure 18) represents each capillary module by a RCL

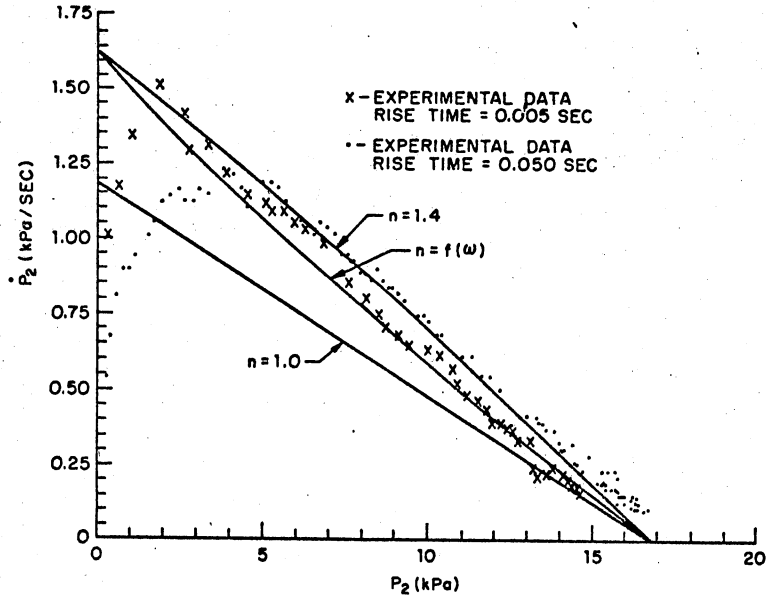

Figure 17. Phase Plane Plots of Enclosed Volume With Pair of Capillaries

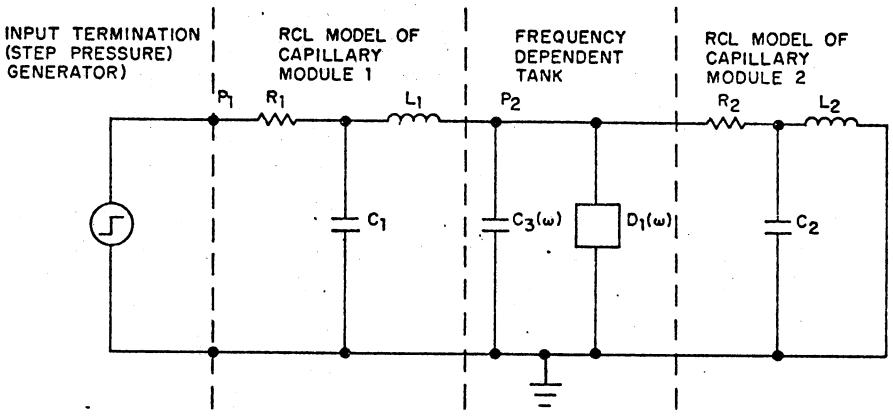

Figure 18. Circuit Diagram for Frequency Dependent Tank With Second Order RCL Models of Capillary Module Terminations

circuit and the tank, by a grounded frequency dependent parallel circuit $[C_3(w)||D_1(w)]$. Here R_i, C_i, and L_i can be linear or nonlinear, frequency independent or dependent.

However, an acceptable first order general circuit is also implemented with a set of loop equations which are defined by one state equation

$$y_1 = \frac{p_1}{R_1} - \frac{y_1}{C_1}\left(\frac{1}{R_1} + \frac{1}{R_2}\right) \tag{3.21}$$

with an initial condition

$$y_1 = 0 \tag{3.22}$$

so that the pressure, p_2, is

$$p_2 = \frac{y_1}{C_1} \tag{3.23a}$$

The pressure rate, p_2, is approximately

$$\dot{p}_2 = \frac{\dot{y}_1}{C_1} - \frac{y_1}{C_1^2}\frac{C_1 - C_1'}{t - t'} \tag{3.23b}$$

where C_1' is the value of C_1 at the last calculated time, t'.

Katz's method for calculating transient response of a frequency dependent tank is adapted for calculating the frequency dependent case. As a first approximation, it appeared appropriate to work closely with Katz's frequency dependent model of the tank and to assume resistive zeroth order model for each of the two capillary models.

A BASIC program was written to calculate the transient solution to the suggested adaptation of Katz's frequency dependent problem for the step response of a capillary and a tank.

Results of transient response computations are presented in conjunction with data as phase plane plots (Figure 17). Here the

simulated network includes linear and nonlinear and frequency independent and dependent models of the tank (enclosed volume) in conjunction with linear and nonlinear 0th order models of the load capillary modules.

Define Error Criteria

Dynamic error criteria are given by equation (2.13b) in Chapter II.

Compute Steady-State and Dynamic Errors

Only dynamic error is considered in these tests. From equation (2.13b) the dynamic error $E(\dot{p}_{max})$ in Figure 17 is computed and tabulated in Table IV.

TABLE IV

COMPARISON OF ERRORS IN EVALUATION OF TANK MODELS

Tank Model			Capillary Model			Penalty Factor	Dynamic Error $E(\dot{p}_{2max})$	Penalized Dynamic Error
Order	C	n	Order	R	L			
1	ℓ	1.0	1	ℓ	ℓ	3	.28	.83
1	ℓ	1.4	1	ℓ	ℓ	3	.01	.04
1	$n\ell$	1.4	0	ℓ	-	3	.01	.04
1	$n\ell$	1.4	0	$n\ell$	-	4	.05	.20
1	ℓ	$f(\omega)$	1	ℓ	ℓ	Reference Model		

Define Penalty Factors

See Table I in Chapter II.

Compute Penalized Steady State and Dynamic Errors

Calculated penalized dynamic errors are given in Table IV.

Select "Best" Model

In contrast to the evaluation procedure for the capillary module earlier in this chapter, a more conclusive position can be taken for the set of lumped models for this tank. Based again upon the selected 1) reference model (the frequency-dependent, linear model, 2) set of simulation models, 3) dynamic error, 4) penalty factors, and 5) test conditions, the "best" model for the tank is a linear capacitor with n = 1.4. It is further seen that nonlinear resistive and capacitive effects are sufficiently small for the linear models of the tank and the capillary module to give adequate results. As in the evaluation procedure for the capillary module, the penalized dynamic error goes through a minimum in the vicinity of the "best" model.

Moving Boundary Confining Structures

A bellows module (Figure 19) (or a diaphragm module) is a mechanical, moving-parts device which is introduced into no-moving fluidic circuits when point-to-point capacitance functions are required. Here two circuit models of the bellows module are discussed, but no complete formulation and evaluation procedure is presented. (Circuit models of a diaphragm module are discussed in reference 21.)

Energy is stored in the bellows module by virtue of deflection of an "elastic" moving member and the fluid compressibility. The

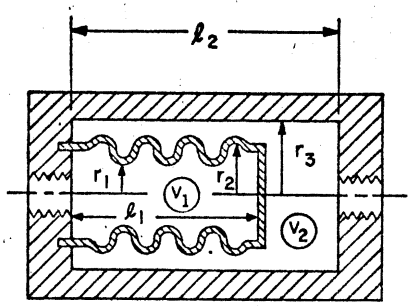

Figure 19. Bellows Module

a)

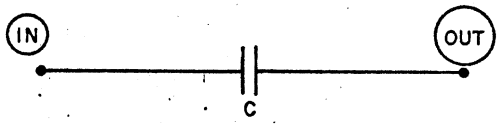

b)

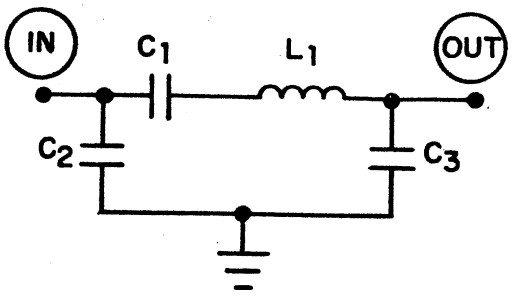

Figure 20. Equivalent Circuit Models for Bellows Module

deflection process is analogous either to mechanical energy being stored in the deflection of a spring or to electrical energy being stored in an electrical capacitor.

The bellows operates approximately in a linear mode as long as its maximum rated deflection, x_{max}, is not exceeded. In a linear operating mode, point-to-point capacitance of the pneumatic bellows module (neglecting fluid compressibility) is

$$C = \frac{A^2}{k} , \tag{3.24}$$

where A is the cross-sectional area of the bellows, and k is the spring rate. Thus, a simple equivalent circuit model of the bellows module is a point-to-point capacitor (Figure 20a).

Real mechanical bellows modules are more complicated, however, and the equivalent circuit (Figure 20b) must contain two grounded capacitors to represent fluid compressibility in the chambers adjacent to the bellows and an inductance to represent inertia of the mass of the bellows. Parasitic resistances might also be expected in an equivalent circuit model of the bellows.

Models of the bellows module are presented for completeness in this chapter. There is no attempt, however, to employ a formal circuit model evaluation procedure as in the case of both the capillary module and the tank. In Chapter V, models of the bellows module are evaluated in a passive lead compensation network by using small-signal a-c frequency response techniques.

CHAPTER IV

COMPUTER-AIDED CIRCUIT ANALYSIS

Digital computer programs are available for calculating network responses of lumped equivalent circuit models of fluidic components. Output responses of fluidic component models may be calculated on a digital computer with state equation solution programs such as FNOL-2 (reference 22) digital simulation programs such as DSL/90 (reference 23) or CSMP and digital circuit analysis programs; e.g., ASTAP, CIRCUS, ECAP, ECAP II, NET-1, NET-2, SCEPTRE, SINC, SLIC, SPICE, and TRAC. These techniques are based on a known circuit model topology and defined values for the circuit model elements (R, L, and C).

Both the state equation programs and the digital simulation languages require as an input a prederived set of differential equations. For large topological structures, formulation of the necessary differential equations can become a major if not untenable undertaking.

A circuit topology and constant element values for R, L, and C can readily be coded into any of the circuit analysis programs. These programs set up internally the requisite circuit equations from the defined topological structure and element values and also solve for the specified form of network response; e.g., d-c, transient, or small signal a-c. However, to date 1) no circuit analysis program has been written exclusively to account for all of the unique features of fluidic circuits, and 2) no single circuit analysis program includes all of the features

necessary for directly implementing all of the unique features of fluidic circuits.

Therefore, an objective of this thesis is to develop a general purpose fluidic circuit analysis program which will afford the user an efficient, versatile tool for analyzing circuits which have components described by nonlinear models with frequency-dependent parameters. Further, this circuit analysis program must, if at all possible, compute simultaneous (rather than computationally delayed) solutions at each selected operating point. It is also desirable that the program be strongly user oriented.

The envisioned digital program would have capabilities 1) of evaluating fluidic component models from the viewpoint of Chapter III; 2) of verifying fluidic component models in the context of systems (as discussed in Chapter V) and finally of optimizing fluidic system designs (as proposed in Chapter VI).

Programs in both FNOL-2 (reference 22) and DSL/90 (reference 23) can be set up to handle the complexities of a circuit definition. Both programs have unique, desirable capabilities and provide simultaneous solutions. However, the versatility of changing circuit topologies is missing in both.

The capabilities of three important circuit analysis programs are tabulated in Table V. SLIC (reference 24) provides simultaneity of solutions but again lacks user flexibility in entering nonlinear models with frequency-dependent parameters since all circuit elements can only be described by numbers rather than parametrically. As a further deficiency, SLIC cannot perform transient analyses.

TABLE V

FEATURES OF SLIC, SCEPTRE, AND NET-2

		(A) SLIC	(B) SCEPTRE	(C) NET-2 Through Release 8
1.	Linear dc	Yes	Yes	Yes
2.	Linear transient	No, but updated version (SPICE) can	Yes	Yes
3.	Linear ac	Yes	No	Yes
4.	Nonlinear dc	Yes; nonlinear resistor has been added at HDL by modifications.	Yes; nonlinear resistor has been added at HDL by new subroutine	Yes; voltage controlled conductance is set in a table to give resistance.
5.	Nonlinear transient	No, but updated version (SPICE) can be modified.	Same as 4B	Same as 4c and a function generator has been defined at HDL for nonlinear capacitors.
6.	Nonlinear ac	Same as 4A but only for small-signal analysis about computed dc operating point.	No	Same as 5c but only for small-signal analysis about computed dc operating point.
7.	Freqency dependent components	Freqency dependent capacitor added at HDL in subroutines	No	Yes
8.	Time dependent components	No, but updated versions (SPICE) can be modified.	Can be added if desired.	Yes
9.	General functions for circuit parameters	Can be added in subroutine.	Can be added if desired.	No, if computational delay is unacceptable; however, any function of one or two variables can be coded as a one- or two-dimensional table, respectively.
10.	Values defined	Numerically	Numerically and analytically	Numerically and analytically
11.	Table look-up	Can be added	Can be added	Yes
12.	General analog simulation blocks	No, but can be added	No, but can be added	Yes
13.	Distributed parameter circuits	May be approximately represented in the frequency domain as phase shift in a lumped element.	May be approximately represented in the time domain as time delay in a lumped element or with Pade approximation.	NOT AT PRESENT Pade approximation for time delay in the complex frequency domain is applied both in small-signal ac and in transient analyses.
14.	Sensitivity analysis	Yes, in updated version of SLIC	Can be added if desired	NOT AT PRESENT
15.	Optimization	Can be added if desired	Can be added if desired	Yes
16.	Simultaneity of solutions	No, solution uses value from last calculated operating point	No, solution uses value from last calculated operating point	Yes
17.	Computer code in terms of fluidic variables and geometries	Can be added if desired	Can be added if desired	NOT AT PRESENT
18.	Model hierarchy defining more complex models, based on simpler defined models	No	Yes	Yes
19.	Computational speed	Adequate	Adequate	Very fast by comparison
20.	Required size of computer	Moderate	Large(depends on the version)	Large
21.	Interactive capability for user to control program as it computes	No	No	No

Four features contribute to the convenience and versatility of NET-2 (reference 25) for studying fluidic circuits. First, nonlinear components may be described in NET-2, so that all response calculations are simultaneous solutions. Second, the values of the elements in the equivalent circuit models may be entered as numbers, as parameters, as algebraic expressions, or as tables. Third, once a subcircuit has been modeled, defined, and arbitrarily named in NET-2, it may be used repeatedly by referring to its name and indicating its connection nodes. Large models may be assembled in NET-2 from both individual element representations and from user-developed models. Fourth, circuit analysis in NET-2 may be performed independently or directly in the context of an optimization. NET-2 performs d-c, small signal a-c, and transient analyses. Increased capability for analyzing fluidic circuits can be introduced through user-developed models at the user level. However, there is almost no possibility for a user to modify NET-2 at a lower level (within the FORTRAN subroutines).

SCEPTRE (reference 26) is a circuit analysis program with approximately the same internal complexity as NET-2, but lacking simultaneity of solutions and self-contained parameter optimization. SCEPTRE cannot perform small signal a-c analysis. Considering the deficiencies of SCEPTRE, the choice was made to work with NET-2 instead of with SCEPTRE.

By selecting the proper structures for user-developed models, the author (reference 18) has developed a fluidic version of NET-2 that allows circuit equations to be solved simultaneously for fluidic structures, modeled in terms of nonlinear resistors, nonlinear capacitors, nonlinear inductors, and nonlinear switching characteristics. Standard

NET-2 elements as well as new model structures are presented and briefly discussed in Appendix B.

In addition, in searching for a circuit analysis program which could be changed at the FORTRAN subroutine level, SLIC was selected. The author has made the necessary modifications to a few FORTRAN subroutines to include nonlinear resistors and frequency dependent capacitors and resistors. Standard SLIC elements as well as new models are presented in Appendix A.

The newly-added computer models make NET-2 extremely versatile in solving nonlinear fluidic equivalent circuits. It is important to recognize that while NET-2 can solve complex systems problems, computation, even if cost-effective, can become very costly. Because of complicated initializing algorithms, simple circuits may in many cases be more costly to solve with NET-2 than with less sophisticated programs such as ECAP or SLIC.

CHAPTER V

EVALUATION OF COMPONENT MODELS USING FREQUENCY RESPONSE TECHNIQUES

It has been shown that based on the evaluation algorithm developed in Chapter II, "best" component can be selected from a set of adequate component models (including a reference model). As demonstrated in Chapter III, the evaluation algorithm is applied in the time domain to several typical large signal equivalent circuit models and method of characteristics models, each with typical termination conditions.

The purpose of this chapter is to demonstrate an alternative viewpoint for a few typical equivalent circuit models of three fluidic components (a capillary module, a tank, and a bellows module from Chapter III) in light of small signal a-c frequency response. Here, only a limited bandwidth, compared to the infinite step response bandwidth in Chapter III, is dealt with. The fluidic components are discussed in two typical component arrays -- a passive summing junction and a passive lead compensation network.

This chapter demonstrates an extension of the approach in Chapter III in terms of features computed from small signal frequency response. However, this chapter is more than an extension of Chapters II and III because it also demonstrates that an intuitive approach, rather than a more highly structured algorithmic approach to modeling,

is quite adequate for selecting plausible "best" component models. Several models (including a reference model for each component) are considered and coded for each component of the fluidic network. Then, simulated responses using several combinations of these models are calculated on a digital computer and compared to experimental responses on the overall fluidic network.

A brief summary of the techniques used for the frequency response measurements precedes discussions of these two passive fluidic networks.

Frequency Response Measurements

Figure 21 is a schematic diagram of the test apparatus used to measure the small-signal frequency response of each physical network. The pressure source was a variable-frequency, sinusoidal pressure generator with very low output impedance. A pair of small microphones, capable of measuring low frequencies and low pressures, monitored pressures at two nodes in the test configuration.

The frequency range was from 1 to 200 Hz and the input pressure amplitude range was from 0.02 kPa (0.003 psi) to 2 kPa (0.3 psi) rms about ambient. There was no net a-c flow.

Passive Summing Junction

A passive fluidic summing junction is designed to produce an output pressure, p_o, which is a function of the sum of input pressures, p_1, p_2, ... (reference 6). The summing junction is composed of a node into which two or more input resistors and a typical load resistor are connected, as shown by the equivalent circuit of Figure 22. Further discussions are limited to a summing junction with three resistors, two

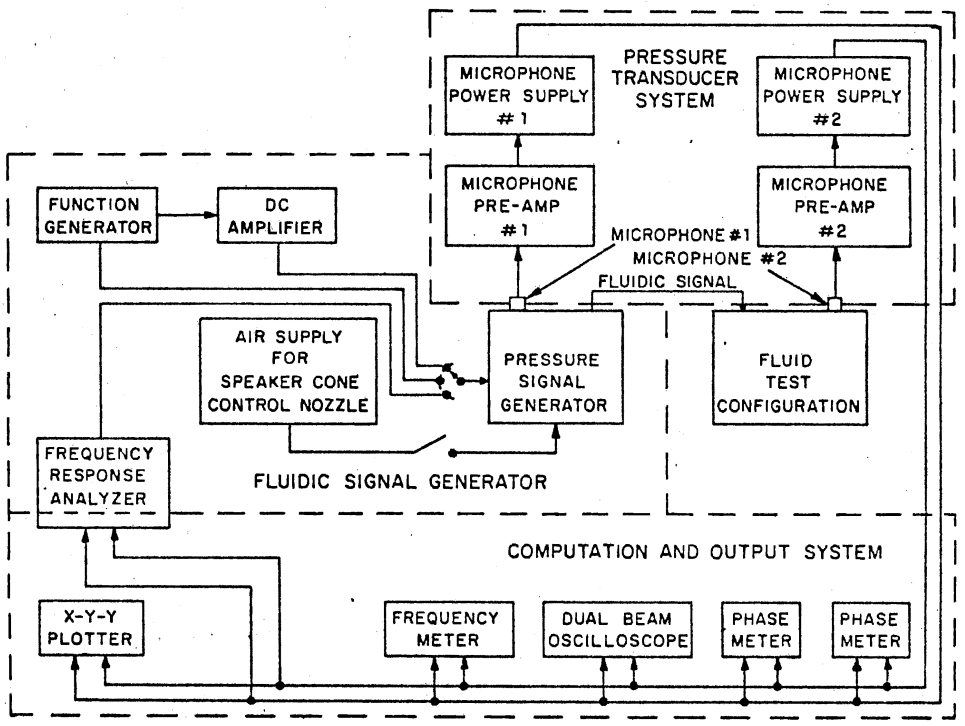

Figure 21. Schematic Diagram of Apparatus for Measuring a-c Fluidic Response

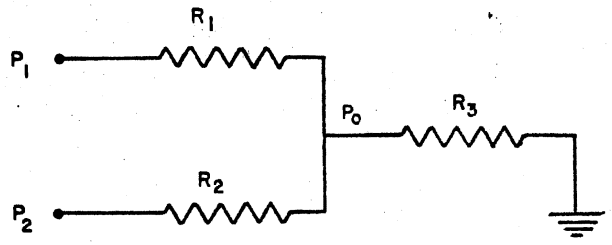

Figure 22. Equivalent Circuit for Loaded Passive Summing Junction

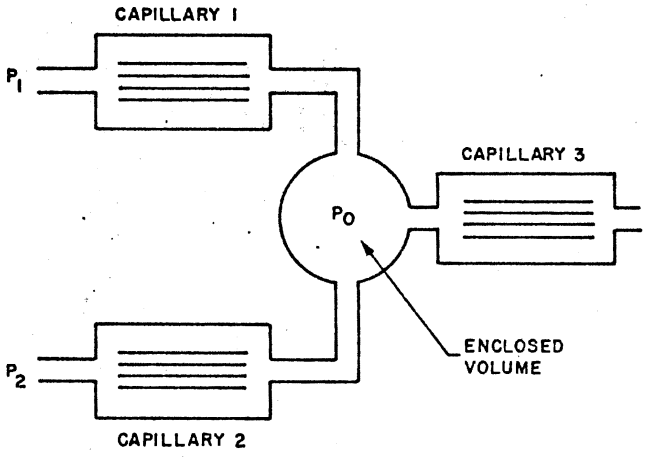

Figure 23. Physical Implementation of the Passive Summing Junction

input resistors, R_1 and R_2, and a load resistor, R_3. Input pressures, p_1 and p_2, are applied to input resistors, R_1 and R_2, respectively. In the special case when $R_1 = R_2 = R_3$, then $p_o = (p_1 + p_2)/3$; that is p_o is independent of the exact values of the resistors.

Figure 23 is a schematic diagram of a physical implementation used to represent the circuit in Figure 22. Capillary modules were used for resistors R_1, R_2, and R_3 and an enclosed volume (tank) was used for the node. For convenience an air cylinder capable of accepting up to five individual connections (Figure 15) was used as the node in the experimental studies. Other parameters were as follows:

Capillary Module 1:

$$N = 25,\ r = 1.525\text{x}10^{-4}\text{m},\ \ell = 0.0635\text{m},\ R_{meas} = 1.07\text{x}10^{8}\ \frac{kg}{m^4\text{-sec}}$$

$$R_{calc} = 2.16\text{x}10^{8}\ \frac{kg}{m^4\text{-sec}},\ L_{calc} = 4.17\text{x}10^{4}\ \frac{kg}{m^4},\ C_{calc} = 8.17\text{x}10^{-13}\ \frac{m^4\text{-sec}^2}{kg}$$

Capillary Module 2:

$$N = 25,\ r = 1.525\text{x}10^{-4}\text{m},\ \ell = 0.0635\text{m},\ R_{meas} = 1.39\text{x}10^{8}\ \frac{kg}{m^4\text{-sec}}$$

$$R_{calc} = 2.16\text{x}10^{8}\ \frac{kg}{m^4\text{-sec}},\ L_{calc} = 4.17\text{x}10^{4}\ \frac{kg}{m^4},\ C_{calc} = 8.17\text{x}10^{-13}\ \frac{m^4\text{-sec}^2}{kg}$$

Capillary Module 3:

$$N = 25,\ 4 = 1.525\text{x}10^{-4}\text{m},\ \ell = 0.0635\text{m},\ R_{meas} = 1.36\text{x}10^{8}\ \frac{kg}{m^4\text{-sec}}$$

$$R_{calc} = 2.16\text{x}10^{7}\ \frac{kg}{m^4\text{-sec}},\ L_{calc} = 4.17\text{x}10^{4}\ \frac{kg}{m^4},\ C_{calc} = 8.17\text{x}10^{-13}\ \frac{m^4\text{-sec}^2}{kg}$$

Volume: $r = 2.54\text{x}10^{-2}\text{m},\ \ell = 1.02\text{x}10^{-2}\text{m}.$

In each case r is the radius, ℓ is length, and R_{meas} is the resistance determined from the steady-state calibration curves (Figure 24). The resistance of each capillary module as computed using the linear portion of equation (3.1) is given by R_{calc}. The measured values of R_1, R_2, and R_3 were used in the model studies in order to minimize the steady-state error.

In a frequency range from 2.5 to 200 Hz with input pressure amplitudes up to 62 Pa (0.010 psi) when parasitics, nonlinearities, and frequency dependencies are considered, the plausible, "best" intuitive models for the fluidic components are as follows:

Capillary modules: linear RLC, $\lambda = 1$, $n = 1.4$

Volume: linear C, $n = 1.4$

Other lumped-parameter models were also considered for the purpose of verifying the choice of a circuit model. An equivalent circuit for the loaded summing junction which incorporates the "best" component models is shown in Figure 25. The three capacitors (which are in parallel) have been combined into one equivalent capacitor; that is

$$C_1' = C_{volume} + C_1 + C_2 \qquad (5.1)$$

Capacitance and inertance values for the circuit elements were calculated from the linear models given by equation (3.3) and (3.4) respectively. Since this study was limited to small-amplitude inputs, the simple linear circuit analysis program, ECAP (reference 27), was selected to compute the frequency response of each equivalent circuit considered.

Bode plots for the linear circuits considered are presented in Figures 26a and b. The theoretical curves A through G are for: 1) capillary modules modeled as R and RLC, 2) for the polytropic coefficient, $n = 1$ and $n = 1.4$, and 3) for the inertance coefficient,

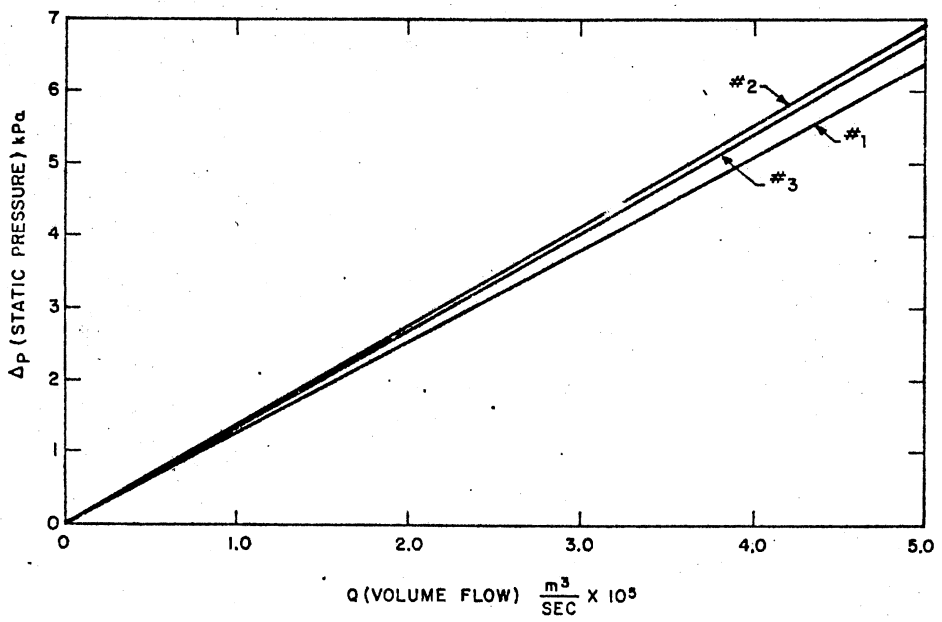

Figure 24. Measured Steady-State Characteristics for the Capillary Modules

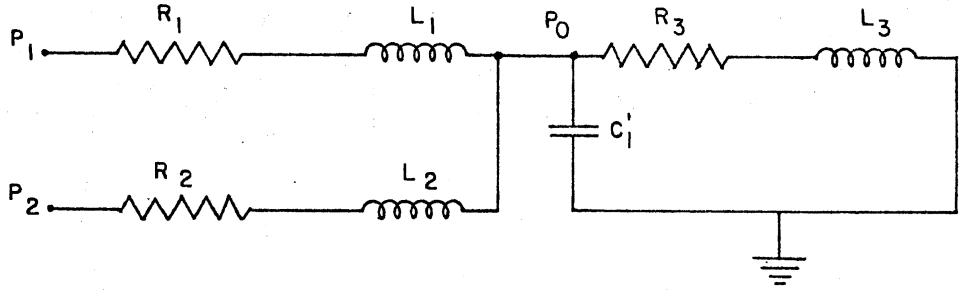

Figure 25. Equivalent Circuit for the Summing Junction With Parasitics

a)

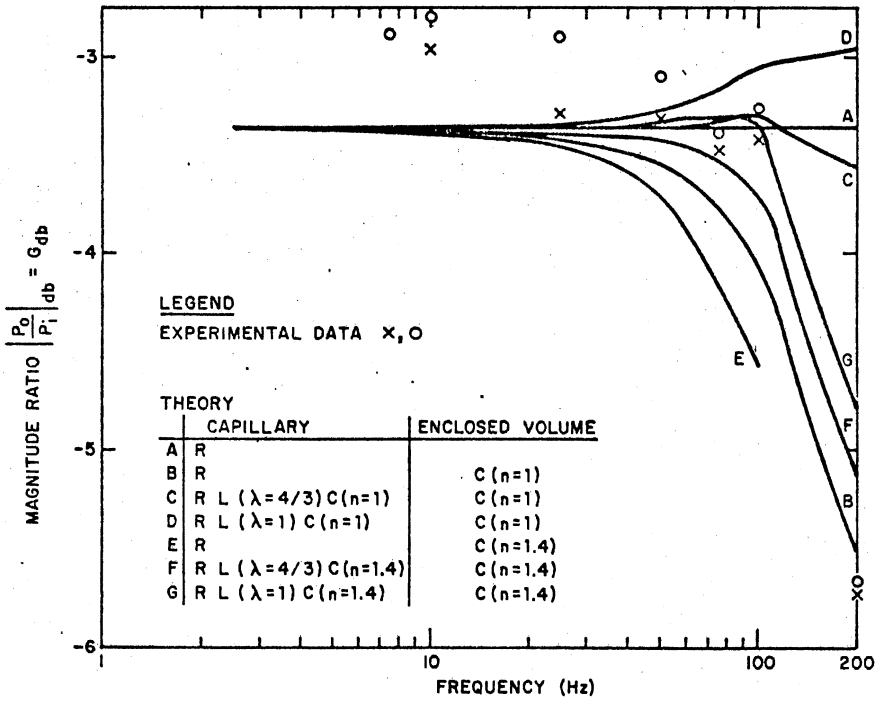

b)

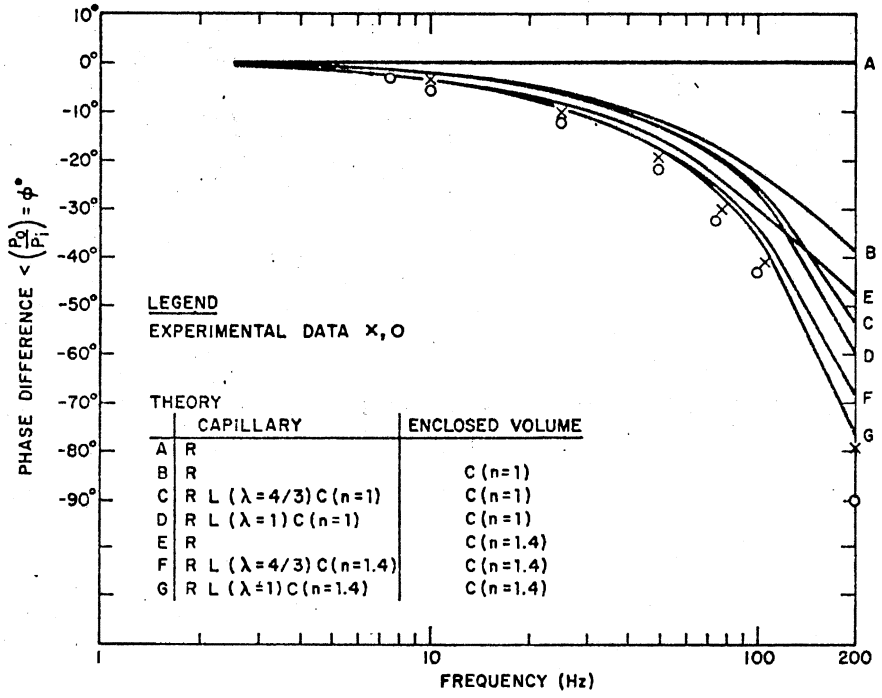

Figure 26. Bode Plot for Summing Junction

$\lambda = 1$ and $\lambda = 4/3$.

The circuit in Figure 23 was tested over a 2.5 to 200 Hz range. The input signals were in phase and of equal amplitude; $|p_1| = |p_2| =$ 0.062 kPa (0.010 psi). Measured magnitude ratios and phase differences (reference 28) are plotted in Figure 26.

The experimental data agrees to within $\pm$ 5% and $\pm 5^{o}$ with curve F for the intuitive "best" models up to 100 Hz. At 200 Hz, experimental data is -10% and -10^{o} different from curve G. The best agreement of simulated and measured frequency response occurs as was expected for the plausible "best" circuit model.

If there were no dynamics in the summing junction, experimental data would agree with curves A (Figures 26a and b) and would be constant over the bandwidth. However from Chapter III, parasitics are known to be produced in both the capillary modules (the input and load resistors) and in the enclosed volume (the node). One conclusion to be drawn from the computed Bode plots (Figure 26) is that the frequency response tests show the capacitance of the node to be the predominant capacitance. Also the choice of n = 1.4 gives considerably better agreement near the corner frequency than n = 1.

Passive Lead Compensation Network

Compensation networks are useful in many control and instrumentation applications. It is possible to implement some useful compensation networks solely with passive fluidic components. The simplest equivalent circuit (Figure 27) for a passive lead network is a point-to-point capacitor, C_1, and a resistor, R_1. Resistor R_2 is a typical resistive load. Figure 28 is a schematic diagram of the physical implementation

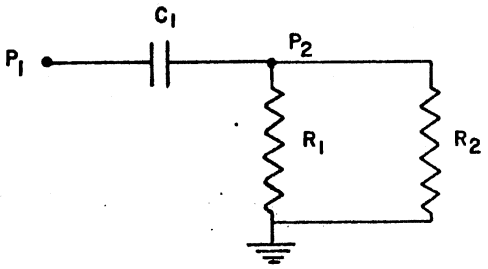

Figure 27. Equivalent Circuit for Loaded Lead Network

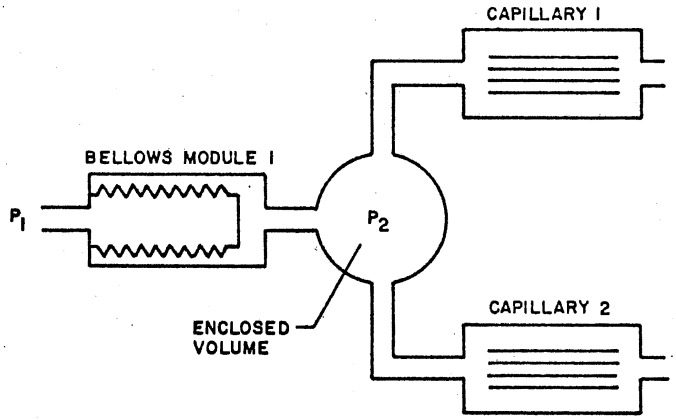

Figure 28. Physical Implementation for Passive Lead Network

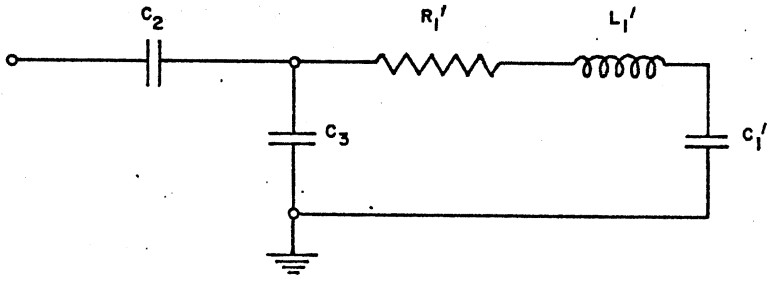

Figure 29. Equivalent Circuit for Lead Network With Parasitics

used to represent the equivalent circuit in Figure 27. The physical components include capillary modules for resistances R_1 and R_2 and a bellows module (Figure 19) for capacitor C_1. An enclosed volume replaces the node at which the bellows module is connected to the capillary modules.

Parameter values for the physical components in the experimental lead circuit in Figure 28 are as follows:

Capillary Module 1:

$$N = 25,\ r = 1.525\times10^{-4}\text{m},\ \ell = 0.08\text{m},\ R = 2.73\times10^{8}\ \frac{\text{kg}}{\text{m}^4\text{-sec}},$$

$$L = 5.26\times10^{4}\ \frac{\text{kg}}{\text{m}^4},\ C = 1.03\times10^{-12}\ \frac{\text{m}^4\text{-sec}^2}{\text{kg}}$$

Capillary Module 2:

$$N = 25,\ r = 1.525\times10^{-4}\text{m},\ \ell = 0.09,\ \text{m},\ R = 3.07\times10^{8}\ \frac{\text{kg}}{\text{m}^4\text{-sec}},$$

$$L = 5.91\times10^{4}\ \frac{\text{kg}}{\text{m}^4},\ C = 1.16\times10^{-12}\ \frac{\text{m}^4\text{-sec}^2}{\text{kg}}$$

Volume: $V = 3.58\ \text{cm}^3$.

Bellows Module: $k = 1.09\times10^{4}\ \frac{\text{kg}}{\text{sec}^2}$, $r_1 = 0.645$ cm, $r_2 = 0.854$ cm,

$r_3 = 0.927$ cm, $\ell_1 = 1.450$ cm, $\ell_2 = 1.777$ cm, $A = 1.25\ \text{cm}^2$,

$V_1 = 1.84\ \text{cm}^3$, $V_2 = 2.96\ \text{cm}^3$.

The permissible maximum deflection (within the elastic limit) was 0.0686 cm.

By an intuitive approach developed from Chapter III, a set of circuit models with minimum adequate complexity to account for nonideal fluidic processes is selected. The plausible "best" intuitive models, in a frequency range between 2.5 and 135 Hz at input pressure of both 1.0 kPa and 2.0 kPa rms above ambient, are as follows:

Capillary modules - linear RLC, $\lambda = 1$, $n = 1.4$, R is measured from the

steady-state calibration curve.

Volume: linear C, n = 1.4

Bellows module: linear capacitances, n = 1.4

As in the case of the summing junction other lumped-parameter models were considered to verify the choice of the circuit models. An equivalent circuit for the physical lead compensation network (Figure 28) includes "best" component models. Four procedures were used to reduce the model structure of this circuit to the equivalent circuit in Figure 29.

1. A Pi network (Figure 20b) was selected as an equivalent circuit model of a bellows module. The horizontal bar of the Pi is a point-to-point capacitor,, C_2, in series with an inductor, L_1. The vertical legs of the Pi are grounded capacitors, C_1 and C_3. When the Pi network of the bellows module is placed at the output of the signal generator, the grounded input capacitor, C_1, which is adjacent to the signal generator, is considered as part of the signal generator. Therefore capacitor, C_1, is neglected in an overall circuit representation of the Pi network.

2. The parallel resistances of capillary modules 1 and 2 are combined so that

$$R_1' = \frac{(R_{\text{capillary 1}}) \times (R_{\text{capillary 2}})}{(R_{\text{capillary 1}}) + (R_{\text{capillary 2}})} \qquad (5.2)$$

3. Similarly the parallel inductances of capillary modules 1 and 2 are so combined that

$$L_1' = \frac{(L_{\text{capillary 1}}) \times (L_{\text{capillary 2}})}{(L_{\text{capillary 1}}) + (L_{\text{capillary 2}})} \qquad (5.3)$$

4. The capacitances of capillary modules 1 and 2 add because they are in parallel so that

$$C_1' = C_{\text{capillary 1}} + C_{\text{capillary 2}} \tag{5.4}$$

Five different equivalent circuits were simulated using the following assumptions.

1. The capillary module models are

A, C) calculated linear R's

B, D) calculated linear R's, linear L's and grounded linear C's;

E) measured R's, linear L's and grounded linear C's.

2. Grounded C's in the node, the bellows module and the capillary modules are

A, B) frequency independent with n = 1.0;

C, D, E) frequency independent with n = 1.4.

Small signal a-c analysis of cases A, B, C, D, and E calculated using NET-2 between 2.5 and 100 Hz are plotted in Figure 30. These plots handle five linear, frequency-independent circuit models.

Both the magnitude ratio plot and the phase-difference plot are modified when the polytropic coefficient is changed from 1.0 (cases A and B) to 1.4 (cases C, D, and E).

A virtually insignificant change can be seen in the magnitude ratio curves by adding L and C to the models of the capillary modules. No change in phase ϕ is noted.

A measured capillary resistance, R (case E) modifies the magnitude ratio curve from the case when the calculated value of R is used (case D).

Frequency was swept from 2.5 to 135 Hz at input pressures of 1.0 kPa (0.15 psi) and 2.0 kPa (0.30 psi) rms about ambient. Experimental

a)

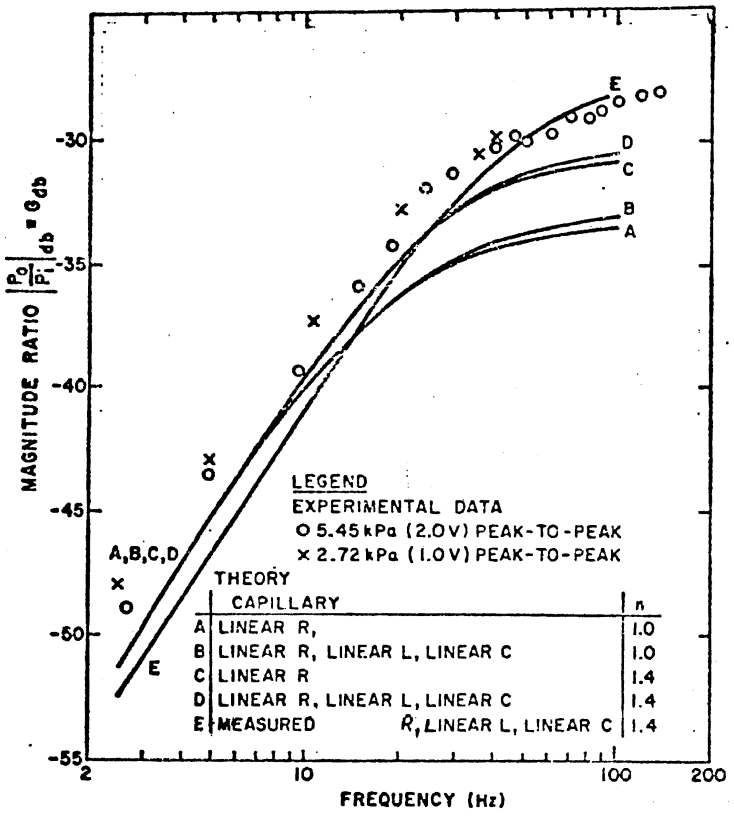

b)

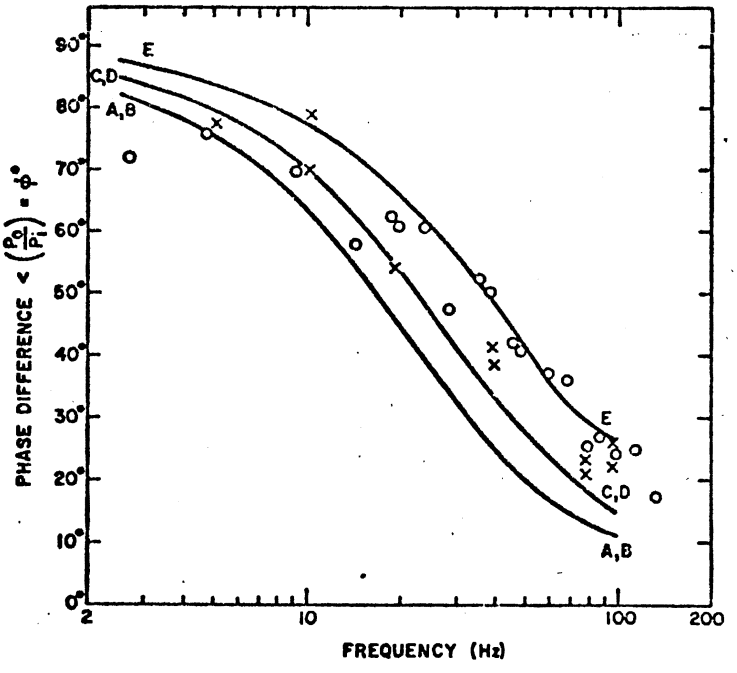

Figure 30. Bode Plot for Lead Network With Bellows

results are presented in a Bode plot (Figures 30a and 30b). Above 10 Hz, experimental data agree within $\pm$ 10% over a 10 db range and within $\pm$ 10^{o} over a 60^{o} range.

The best agreement occurs in frequency response between experimental and simulated data from the plausible "best" models, as was expected.

CHAPTER VI

DESIGN APPROACH TO FLUIDIC CONFIGURATIONS

The methods discussed for synthesizing circuit models of fluidic components are directed toward the specific goal of providing valid circuit models for designing fluidic systems. A particular fluidic component can be modeled by one of several equivalent circuits, each predicting a valid circuit response over a specific operating range and within a specified static and dynamic error. It is possible to conceive of a catalog of circuit models of passive fluidic components which will be defined in terms of:

1. Topological arrays of energy dissipation and storage elements.
2. Values of circuit elements in an array defined as constants, parametrically, or as variables (dependent on pressure, flow, time or frequency). Element values may be defined in either open or closed form in terms of parameters which are bounded or unbounded and discrete or continuous.
3. Operating ranges given for bandwidth and pressure amplitude.
4. Mean or maximum static and dynamic response errors specified over the operating ranges.

It is possible to envision a fluidic circuit design approach which is valid within the ranges in which the fluidic circuit models are cataloged. Such an approach, suggested in Figure 31, consists of both basic

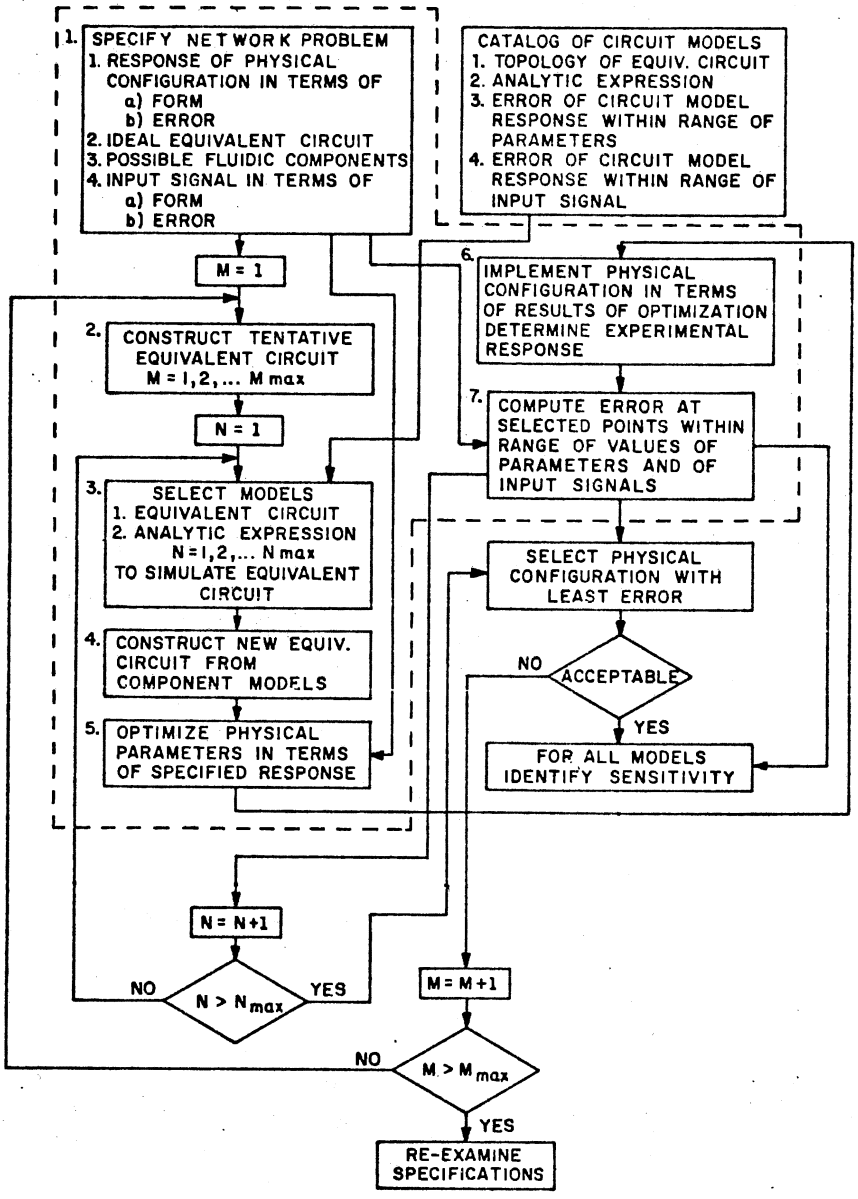

Figure 31. Flow Chart of Design Approach

design (within the dashed lines) and peripheral circuit model improvements. The approach is:

1. Specify the system design problem (including the desired dynamic response),
2. define an ideal equivalent circuit,
3. select real fluidic components whose circuit models contain first order effects which match the ideal equivalent circuits,
4. define new equivalent circuits which contain important parasitic effects,
5. adjust (optimize) parameters of the circuit models such that design specifications are met while still maintaining a physically realizable configuration,
6. implement the circuit defined in 3 and 5 and measure the dynamic response,
7. compare measured and desired response, and
8. iterate on steps 1 to 7 as required or desired.

Specification of the System Design Problem

Specification of the system design problem is made in terms of a required output nodal response of the physical configuration. One or more required aspects of the nodal response are specified as a value plus or minus an error. Standard forms of nodal response such as steady-state d-c response, steady-state a-c response, and transient response should be employed. Steady-state d-c response is defined by attenuation ratios between nodes. Critical aspects in defining steady-state a-c nodal response may be given through performance criteria in the complex frequency domain based on values of gain margin, phase

margin, bandwidth, peak resonance, and break frequencies. Transient nodal response, observed through performance criteria in the time domain, may be based on values of rise time, delay time, settling time, and overshoot.

Construction of an Ideal Equivalent Circuit

One of several simple circuits that might produce the general form of the desired response can be synthesized. The lowest order ideal circuit that satisfies the form of the response should be selected. Many texts and references such as Chestnut and Mayer (reference 29) present tables of low-order circuit topologies with their nodal response.

Selection of Fluidic Components

The set of passive fluidic components that can be used in these designs might include orifices, area changes, and transmission lines, as well as those discussed in Chapter III (capillary modules, enclosed volumes, bellows modules).

The existing model catalog will be checked for components that, over the specified operating ranges, represent the specified forms of pure resistance, pure inductance, and pure capacitance. For example, a linear resistor might be implemented by a capillary, a point-to-point capacitor by a bellows module or a diaphragm module, and a grounded capacitor by an enclosed volume.

Definition of New Equivalent Circuits Representing Real Fluidic Components

The basic ideal equivalent circuit can now be developed into a new equivalent circuit which includes important parasitic effects. For example, for some operating ranges, a linear resistor that is implemented by a fluidic capillary might be represented by an RLC circuit model. Because secondary as well as primary effects occur in many components in the ranges of interest, certain circuit functions may be nonrealizable with the available passive components.

Equivalent circuit models can be coded into one of the digital computer-aided circuit design programs, in which circuit simulations and circuit parameter optimizations can be performed.

Adjustment (Optimization) of Parameters to Fulfill Specifications

There are two possible approaches for obtaining satisfactory agreement between the desired and simulated responses. First, the element values or the parameters within expressions defining the element values, may be adjusted. Second, the circuit topology may be changed.

A computerized circuit parameter optimization procedure, such as that contained within NET-2, automatically minimizes the error between the simulated and specified desired responses as a function of the design parameters. One possible form of error (or performance) criteria in a design is the integrated least squares difference between the simulated and desired frequency responses.

It is impossible in many cases to adjust parameters in a given circuit simulation to produce the desired response. Difficulties arise

because compatibility cannot be achieved among the desired response, the allowable fluidic component structures, and the selected circuit topology. Nonrealizability of certain parameter values of the fluidic components will introduce this.

System Implementation and Dynamic Response Measurement

To validate the design procedure, a fluidic system can be implemented on the basis of the required topology. Specified sources and loads are connected to the system terminals and pressure measurements are taken simultaneously at a pair of nodes. Results are plotted in convenient forms.

Comparison of Measured and Desired Responses

Performance criteria are scalar values that define errors between measured and specified responses. For example, performance criteria might be mean or maximum static and dynamic errors between measured and desired responses.

Iterations of Design Approach

After sufficient iterations, the design approach should result in selection of fluidic hardware which meets the specified design criteria.

SELECTED BIBLIOGRAPHY

(1) Kirshner, Joseph M. Fluid Amplifiers. New York: McGraw-Hill Co., 1966.

(2) Blackburn, John F., Gerhard Reethof, and J. Lowen Shearer. Fluid Power Control. Cambridge, Mass.: MIT Press, 1960.

(3) White, Harry N. "Analysis of the Steady-Flow Pneumatic Resistance of Parallel Capillaries." Proceedings of the Fluid Amplification Symposium, Volume 1. Washington, D.C.: Harry Diamond Labs, October, 1965.

(4) Merritt, Herbert E. Hydraulic Control Systems. New York: Wiley, 1967.

(5) Rohman, C. P., and E. C. Grogan. "On the Dynamics of Pneumatic Transmission Lines." Transactions of the ASME (May, 1957), 853-874.

(6) Turnquist, Ralph O. "Fluerics (Fluid Amplification), 18. A Fluid State Digital Control System." Washington, D.C.: HDL, February, 1966.

(7) Katz, Silas, and Edgar Hastie. "Fluerics 31. The Transition from Isothermal to Adiabatic Capacitance in Cylindrical Enclosures." Washington, D.C.: HDL-TM-71-35, Harry Diamond Labs, 1971.

(8) Katz, Silas, and Edgar Hastie. "Pneumatic Passive Lead Networks for Fluidic Systems." Joint Automatic Control Conference, St. Louis, 1971.

(9) Belsterling, Charles A. Fluidic Systems Design. New York: Wiley-Interscience, 1971.

(10) Manion, F. M. "Dynamic Analysis of Flueric Proportional Amplifier." ASME Paper No. 68-FE-49. New York: ASME, December, 1968.

(11) Reid, Karl N. "Fluid Transmission Lines." Stillwater, Oklahoma: School of Mechanical and Aerospace Engineering, Oklahoma State University, July-August, 1968.

(12) Shearer, Jesse L., Arthur T. Murphy, and Herbert H. Richardson. Introduction to System Dynamics. Reading, Mass.: Addison-Wesley, 1967.

(13) Harry Diamond Labs Staff. "Fluerics 23. A Bibliography." Washington, D.C.: HDL-TR-1495 (RA), October, 1971.

(14) Boyle, Graeme R., Barry M. Cohn, and Donald O. Pederson. "Macromodeling of Integrated Circuit Operational Amplifiers." IEEE Journal of Solid-State Circuits, Vol. SC-9, No. 6 (December, 1974), 353-364.

(15) Lindholm, Fredrik A. "Device Characterization for Computer Analysis of Large Circuits." IEEE Trans. on Nuclear Science, Vol. NS-18, No. 6 (December, 1971), Electrical Engineering Department, University of Florida, Gainesville, Florida, 206-211.

(16) Happ, William W., and John Staudhammer. "Topological Techniques for the Derivation of Models with Pre-Assigned Accuracy." Archiv Der Elektrischen Ubertragung, Vol. 20, No. 6 (1966), 329-335.

(17) Kirshner, Joseph M., and Silas Katz. Design Theory of Fluidic Components. New York: Academic Press, 1975.

(18) Iseman, Joseph M. "Computer-Aided Fluidic Circuit Analysis and Design." Proceedings of the HDL State-of-the-Art Fluidics Symposium. Washington, D.C.: Harry Diamond Labs, October, 1974.

(19) Hausner, Arthur. Analog and Analog/Hybrid Computer Programming. Englewood Cliffs, N.J.: Prentice Hall, Inc., 1971.

(20) Zalmonzon, L.A. Components for Pneumatic Control Instruments. Oxford: Pergamon, 1965.

(21) Iseman, Joseph M. "A Circuit Analysis Approach to the Solution of Passive Pneumatic Fluidic Compensation Networks." Proceedings of the HDL State-of-the-Art Fluidics Symposium. Washington, D.C.: Harry Diamond Labs, October, 1974.

(22) Linnekin, Jerry S., and L. J. Belliveau. "FNOL2, A Fortran (IBM 7090) Subroutine for the Solution of Ordinary Differential Equations with Automatic Adjustment of the Interval of Integration." Mathematics Department Report M-38. White Oak, Maryland: U.S. Naval Ordnance Laboratory, July 17, 1963.

(23) Bloom, H.M. "DSL/90 Programming Manual." HDL-TM-7113, Washington, D.C.: Harry Diamond Labs, October, 1971.

(24) Kop, Harold M. "An Improved Version of SLIC." Memorandum No. ERL-M364 Electronics Research Laboratory. Berkeley: College of Engineering, University of California, August 3, 1972.

(25) Malmberg, Allan F. "Preliminary User's Manual, NET-2 Network Analysis Program." Washington, D.C.: Harry Diamond Labs, September, 1972.

(26) Mathers, Harry W., Stephen R. Sedore, and John R. Sents. "SCEPTRE Support, Volume 1: Revised SCEPTRE User's Manual." Technical Report No. AFWL-TR-67-124, Vol. 1. Kirtland AFB, N.M.: Air Force Weapons Laboratory, April, 1968.

(27) Anon. "ECAP, 1620 Electronic Circuit Analysis Program." Report No. H20-0170-1. White Plains, N.Y.: IBM Corp., 1965.

(28) White, Dyrull V. "Pneumatic Fluidic Summing and Distribution Junctions." Proc. Student Trainee Technical Symposium. Washington, D.C.: Harry Diamond Labs, 1973.

(29) Chestnut, Harold, and Robert W. Mayer. Servomechanisms and Regulating System Design, Vol. II. New York: Wiley, 1955.

(30) Chua, Leon O. Introduction to Nonlinear Network Theory. New York: McGraw-Hill Book Co., 1969.

APPENDIX A

FLUIDIC CIRCUIT MODELS IN SLIC

SLIC (reference 24) is a simple, inexpensive to execute program that is primarily useful for linear a-c circuit analyses. Simple modification (reference 18) of a few FORTRAN subroutines makes it possible to model 1) resistors with first-order dependence on pressure drop and 2) resistors and capacitors with frequency-dependent parameters. SLIC is available from Electronics Research Laboratory, College of Engineering, University of California, Berkeley, California. A complete listing for SLIC including the fluidics modifications is available from Chief, Fluid Systems Research Branch, Harry Diamond Laboratories, Adelphi, Maryland 20783.

Standard Element Models in SLIC

The standard elements in SLIC which are used in a fluidic circuit analysis package are linear voltage sources, linear current sources, linear resistors, linear capacitors, and linear inductors (Table VI).

Nonlinear Resistance in SLIC

In version C-3 of SLIC (reference 24), the values of the nonlinear resistors are computed directly as the elements of the admittance matrix is formed. In the subroutine DCANAL (for d-c analysis) the nonlinear resistance, R, is of the form of equation (3.1):

$$R = R_{\ell} \sqrt{1 + \frac{2R_q}{R_{\ell}^2} \Delta p} \qquad (A.1)$$

TABLE VI

STANDARD ELEMENTS IN SLIC (VERSION C-3)

Element	Input Card Format			
1. Voltage source	Vn	a	b	Value
2. Current source	In	a	b	Value
3. Resistor	Rn	a	b	$x_r y_r z$
4. Capacitor	Cn	a	b	$x_c y_c z$
5. Inductor	Ln	a	b	Value

where

a = input node number

b = output node number

n = alphanumeric name designating a particular element

and for

z = 0 (the frequency-independent case)

x_r = linear value of resistance

x_c = linear value of capacitance

and for

z = 1 (the nonlinear resistance case)

x_r = linear value of resistance

y_r = coefficient of first-order term of resistance

and for

z = 2 (the frequency-dependent case)

$z_r = x_c$ and is the value of capacitance as frequency approaches zero

$y_r = y_c$ and is the radius of a cylindrical enclosed volume

The value of R is iteratively calculated until the same value occurs for three successive calculations.

Nonlinear resistors are coded as data into SLIC through the resistor element card, which is of the form

Rn a b x y z

where n is an alphanumeric resistor name, a and b are the node numbers between which the resistor is connected, and z = 1 indicates that the resistor is of the nonlinear form (equation A.1).

$$x = R_{\ell}, \tag{A.2a}$$

$$y = R_{q}, \tag{A.2b}$$

$$z = 1 \tag{A.2c}$$

Frequency-Dependent Capacitance and Resistance in SLIC

The frequency-dependent capacitor is implemented in new subroutines called by the subroutine ACANAL (for a-c analysis). The cylindrical frequency-dependent enclosed volume (Chapter III) is shown to be a capacitor $C = C(\omega)$ shunted by a resistor $R = D(\omega)$, as described in equations (3.17a, b).

The frequency response analysis is initiated in the subroutine ACANAL as the desired frequency range is swept. If the capacitor-resistor pair is frequency dependent, then the values of $C(\omega)$ and $D(\omega)$ are calculated in special fluidic subroutines FDVOLC and FDVOLR, respectively.

The frequency-dependent capacitor-resistor pair is coded into SLIC as data on a capacitor card and a resistor card of the form

Cm a b x y z

Rn a b x y z

where m and n are alphanumeric names of the capacitor and resistor, respectively, a and b are the numbers of the nodes between which the parallel capacitor-resistor pair are connected, x is the capacitance value of an identical capacitor for the adiabatic case

$$x = \frac{V}{\gamma p_{\infty}} \tag{A.3}$$

y is the radius of the cylindrical volume, and z is 2. Here, V is the volume of the cylindrical volume, p_{∞} is the reference static pressure, and γ is the ratio of specific heats.

When z = 2, the SLIC program treats the capacitance and resistance as frequency-dependent components.

APPENDIX B

FLUIDIC CIRCUIT MODELS IN NET-2

NET-2 (reference 25) is a sophisticated network analysis program which has the versatility of computing d-c, transient, and small signal a-c responses. The framework provided in NET-2 for obtaining simultaneous solutions for circuits in which element values are functionally dependent on response variables is presented below. Then in the next section, the author demonstrates the technique he has developed for coding 1) functionally dependent resistors, 2) functionally dependent capacitors, 3) functionally dependent inductors, and 4) functionally dependent switches into NET-2. Availability of NET-2 including fluidics modifications may be ascertained through requests to Chief, Fluid Systems Research Branch, Harry Diamond Laboratories, Adelphi, Maryland 20783.

Standard Elements in NET-2

A total of 16 elements of current interest are available in NET-2, release 8 (reference 25). Each of the standard elements is designated both by a type name and by a number for that type. The nodes to which it is connected and its value are specified. Table VII summarizes the standard NET-2 elements.

Basic Functionally Dependent Components in NET-2

In NET-2 functionally dependent quantities can be written directly into the expressions that define the "value" of the components. If the "value" is defined by an expression which is a function of a response variable, simultaneity of solution will be sacrificed. However, by using the simulation elements (7-12, Table VII) in conjunction with the voltage controlled elements (13-16, Table VII), the functionally dependent expressions may be rephrased so that simultaneous solutions are obtained.

TABLE VII

STANDARD ELEMENTS IN NET-2 (RELEASE 8)

Element name	NET-2 coding format	
1. Voltage source	Vn	a b Value, r
2. Current source	In	a b Value
3. Resistor	Rn	a b Value
4. Capacitor	Cn	a b Value
5. Inductor	Ln	a b Value
6. Switch	Sn	a b Value
7. Gain block	GAINn	a b Value
8. Summer	SUMn	b $\pm a_1$ $\pm a_2$ . . .
9. Integrator	INTn	a b g
10. Differentiator	DERIVn	a b
11. Multiplier	MULTn	b $\pm a_1$ $\pm a_2$ . . .
12. Limiter	LIMn	a b Value
13. Voltage controlled conductance	VCGn	e f a b g
14. Voltage controlled voltage source	VCVSn	e f a b g, r
15. Voltage controlled current source	VCCSn	e f a b g
16. Voltage controlled conductance defined by table look-up	XMODn	8 1 a b //TABLEm

where a, a_1 are input node names
b is an output node name
e, f are differential control node pairs
g is a gain value
m is a number designating a particular table
n is a number designating a particular element
r is the value of internal resistance

Functionally Dependent Resistor

A functionally dependent resistance value that occurs frequently in fluidic components has the form

$$R = f(Q) \tag{B.1}$$

A resistor of this form is implemented computationally in NET-2 with a voltage-controlled conductance (VCG). The schematic is given in Figure 32.

Resistance is established in VCG1. The flow is metered in R1 and evaluated at node 3. Functions are introduced at node F. The conductance, calculated and evaluated at node 10, is applied to VCG1 between node pair 10 and 0.

A typical defined model, designated as RFVCG (Resistance, Functionally dependent with a VCG), is shown in Figure 32 and Table VIII.

TABLE VIII

NET-2 LISTING OF FUNCTIONALLY DEPENDENT RESISTOR, RFVCG

```
DEFINE    RFVCG     IN    OUT   0     F
   R1     IN   1    SMALL METERING RESISTANCE, E.G., .001
   VCG1   10   0    1     OUT, 1.
   SUM1   2    +IN  -1
   GAIN1  2    3    1./R1
```

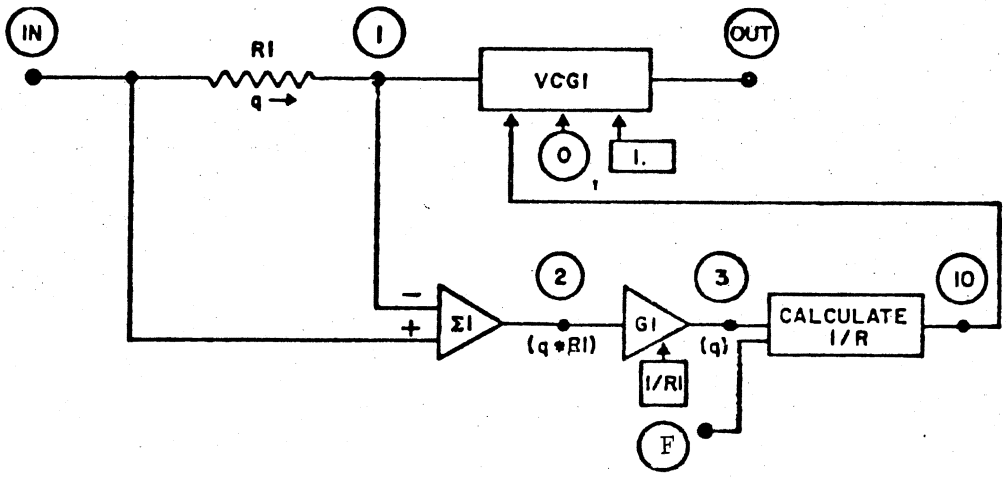

Figure 32. Functionally Dependent Resistor

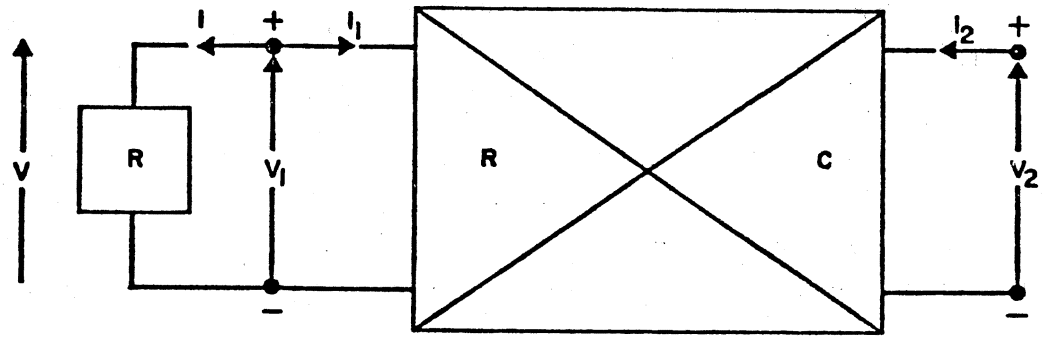

Figure 33. Nonlinear Capacitor Using Type-1 RC Mutator

Functionally Dependent Point-to-Point Capacitor (Using Type-1 RC Mutator)

A functionally dependent point-to-point capacitor is modeled as a type-1 RC mutator (Chua, reference 30). A mutator is in the class of a more general two-port (four terminal) device -- the gyrator. In essence, voltage and current functions may be interchanged within the gyrator.

To form a nonlinear point-to-point capacitor, C, with the same value as $\frac{k}{R}$ (where k = 1 in units of time), a type-1 RC mutator is used. A functionally dependent resistor, R, is used, as well as controlled-voltage sources and controlled-current sources. The RC mutator is a two-port black box (Figure 33).

For the resistor, R, Ohm's law gives

$$v = Ri \tag{B.2a}$$

where

$$v = v_1 \tag{B.2b}$$

and

$$i = -i_1 \tag{B.2c}$$

so that

$$v_1 = -Ri_1 \tag{B.2d}$$

A capacitance-type relationship between v_2 and i_2 is required so that

$$v_2 = \frac{1}{C} \int i_2 \, dt \ . \tag{B.3}$$

Equating $\frac{1}{C}$ and $\frac{R}{k}$ in equations (B.3) and (B.2d) gives

$$\frac{1}{C} = \frac{R}{k} \tag{B.4a}$$

and substituting for $\frac{1}{C}$ from the integral equation (B.3) and R from equation (B.2d).

$$\frac{v_2}{\int i_2 \, dt} = \frac{v_1}{-ki_1} \quad . \tag{B.4b}$$

Then the numerators of equation (B.4b) may be equated and the denominators of equation (B.4b) may be equated:

$$\begin{cases} v_2 = v_1 & \text{(B.4c)} \\ \int i_2 \, dt = -ki_1 & \text{(B.4d)} \end{cases}$$

Differentiating equation (B.4d) with respect to t gives the pair of equations:

$$\begin{cases} v_1 = v_2 & \text{(B.5a)} \\ i_2 = -k \frac{di_1}{dt} & \text{(B.5b)} \end{cases}$$

Thus, relationships for a type-1 RC mutator have been derived. In Figure 34, R can be driven by a controlled-voltage source, $v_1 = v_2$, and $\frac{1}{C}$ can be driven by a controlled-current source, $i_2 = -k \frac{di_1}{dt}$. The value of $\frac{1}{C}$ can from (B.4a) be set equal to the value of $\frac{R}{k}$ (where k = 1).

The NET-2 model that simulates this functionally dependent capacitor is shown in Figure 35. The main body of this RC mutator is the voltage-controlled voltage source, VCVS1, and the voltage-controlled current source, VCCS1. The calculated functionally dependent value, C, is introduced at node F. The voltage-drop relationship between V_{IN} and V_{OUT}, that is implemented as the output of SUM1 at node 1 (referenced to ground), controls VCVS1. The relationship between i_1 and i_2 is set up

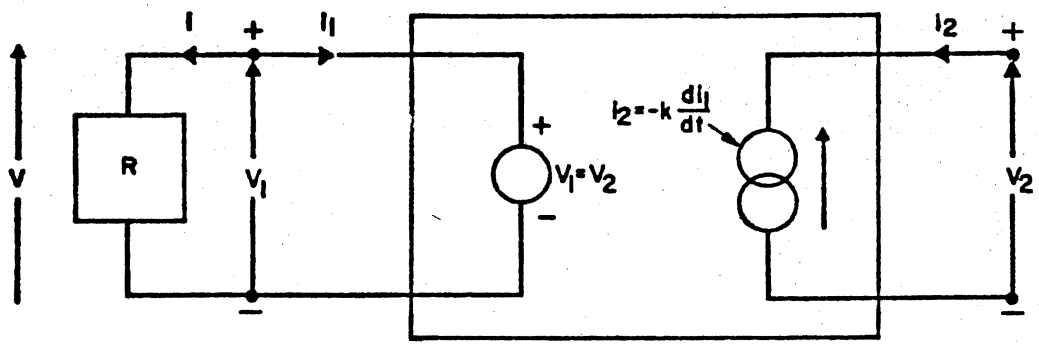

Figure 34 . Schematic of Type-1 RC Mutator as Capacitor

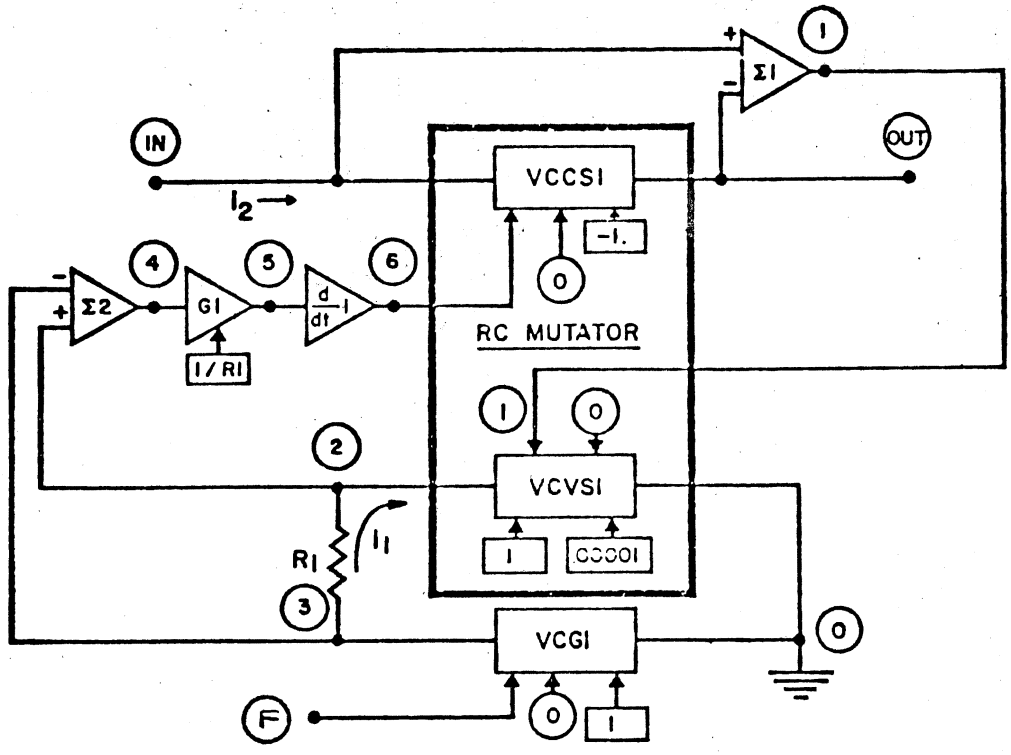

Figure 35. Functionally Dependent Capacitor (Using Type-1 RC Mutator)

by metering the input current into VCVS1 with resistor R1, calculating i_1 with SUM2 and GAIN1, and differentiating it in DERIV1. Node 6 at the output of DERIV1 (referenced to ground) controls VCCS1.

The element VCCS1 in this mutator serves as the functionally dependent capacitor. In Figure 35 and Table IX, the functionally dependent point-to-point capacitor (defined as a model in NET-2) is called CFPP (Capacitance, Functionally dependent, Point-to-Point).

TABLE IX

NET-2 LISTING OF FUNCTIONALLY DEPENDENT CAPACITOR, CFPP

```
DEFINE    CFPP       IN    OUT   0     F
    VCCS1 6    0     IN    OUT   -1.
    SUM1  1    +IN   -OUT
    VCG1  NL   0     3     0     1.
    VCVS1 1    0     2     0     1. SMALL_INTERNAL RESISTANCE,
                                     E.G., .00001
    R1    2    3     SMALL METERING RESISTANCE, E.G., .001
    SUM2  4    +2    -3
    GAIN1 4    5     1./R1
    DERIV1 5   6
```

Functionally Dependent Inductor (Using Type-1 RL Mutator)

A functionally dependent inductor also is modeled as a mutator. For the functionally dependent inductor, a type-1 RL mutator (Chua, reference 30) is modeled. Starting with a functionally dependent resistor, R, and using the type-1 RL mutator, a functionally dependent inductor, L, equal to kR (where k is unity in units of time) is to be constructed. The RL mutator is considered as a two-port black box (Figure 36).

An Ohm's law relationship between the voltage drop, v, and the current, i, is

$$v = Ri \tag{B.6a}$$

where

$$v = v_1 \tag{B.6b}$$

and

$$i = -i_1 \tag{B.6c}$$

so that

$$v_1 = -Ri_1 \tag{B.6d}$$

The RL mutator must be designed to develop an inductive type relationship between v_2 and i_2, as

$$v_2 = L \frac{di_2}{dt} \tag{B.7a}$$

or

$$v_2 \, dt = L di_2 \tag{B.7b}$$

where L and kR in equations (B.7a) and (B.6d) have the same value. That is

$$L = kR \tag{B.8a}$$

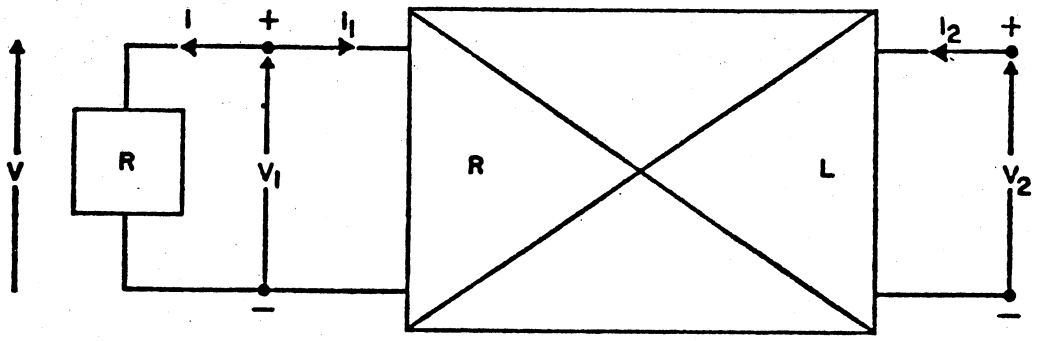

Figure 36. Nonlinear Inductor Using Type-1 RL Mutator

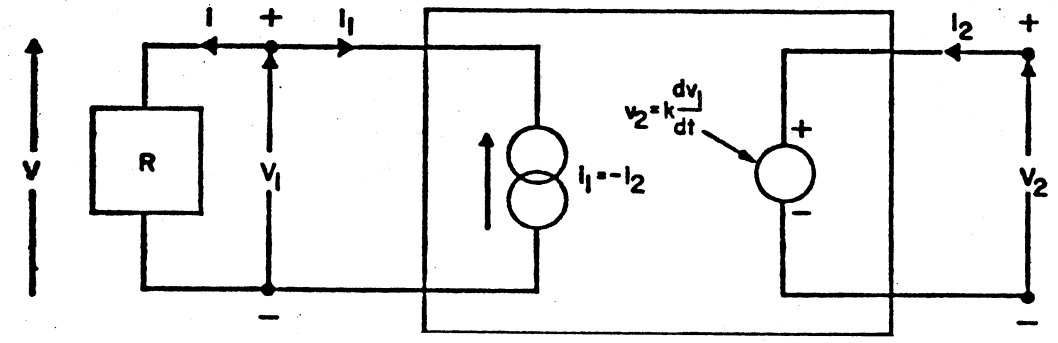

Figure 37. Schematic of Type-1 RL Mutator as Inductor

Substituting for R from equation (B.6d) and for L from equation (B.7a), yields

$$\frac{\int v_2\,dt}{i_2} = -\frac{kv_1}{i_1} \quad . \tag{B.8b}$$

Both the numerators of equation (B.8b) may be equated and the denominators of equation (B.8b) may be equated

$$\begin{cases} \int v_2\,dt = kv_1 & \text{(B.8c)} \\ i_2 = -i_1 & \text{(B.8d)} \end{cases}$$

Differentiating equation (B.8c) with respect to t gives the pair of equations

$$\begin{cases} v_2 = k\,\dfrac{dv_1}{dt} & \text{(B.9a)} \\ i_1 = -i_2 & \text{(B.9b)} \end{cases}$$

Equations (B.9a) and (B.9b) are the necessary relationships for a type -1 RL mutator. As shown in Figure 37, R can be driven by a controlled-current source, $i = i_2$, while L can be driven by a controlled voltage source, $v_2 = k\,\dfrac{dv_1}{dt}$. The value of L can therefore be equated to the value of R (where $k = 1$). A NET-2 simulation model of this functionally dependent inductor is shown in Figure 38.

The mutator itself is a voltage-controlled voltage source, VCVS1, and a voltage-controlled current source, VCCS1. Node F is set at a voltage corresponding to the reciprocal of the value of the functionally dependent inductor, 1/L. The value of i_1 is set by metering the current i_2 through R1 with SUM1 and GAIN1. Node 3 at the output of GAIN1 controls VCCS1, which has the gain of 1.0. The relationship between V_2 and V_1 is calculated with DERIV1, the output of which (node 5) controls VCVS1. In this mutator, VCVS1 serves as the nonlinear inductor.

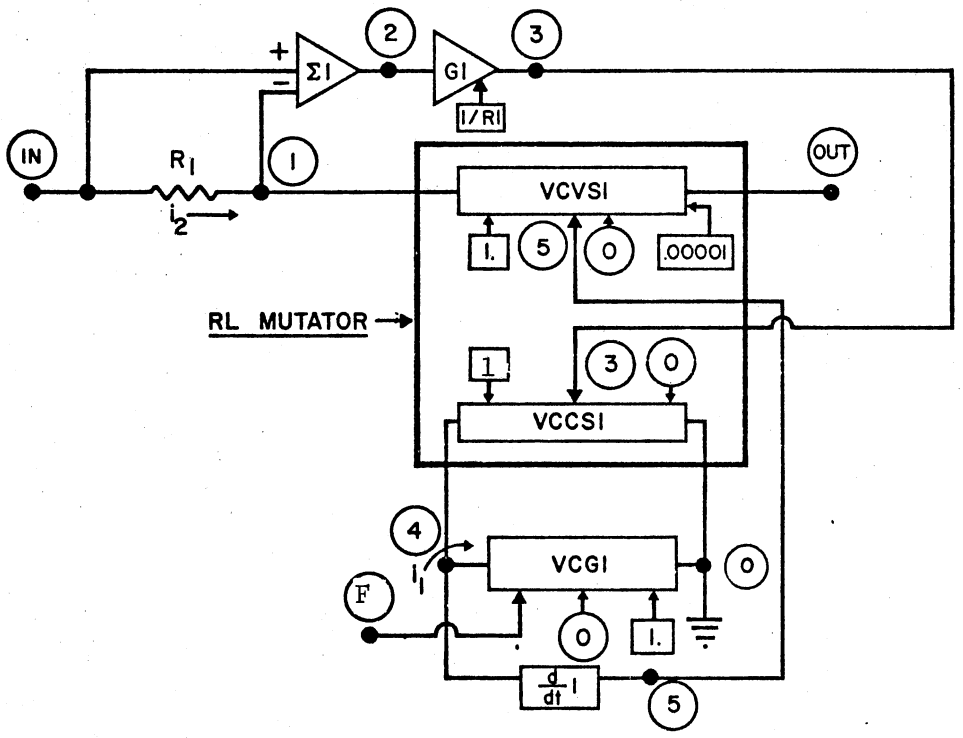

Figure 38. Functionally Dependent Inductor (Using Type-1 RL Mutator)

The functionally dependent inductor (Figure 38 and Table X) is defined as the model, LF (Functionally dependent inductor (L)).

TABLE X

NET-2 LISTING FOR FUNCTIONALLY DEPENDENT INDUCTOR, LF

```
DEFINE    LF        IN   OUT  0     F
   R1     IN   1    SMALL METERING RESISTANCE, E.G., .001
   SUM1   2    +IN  -1
   GAIN1  2    3    1./R1
   VCVS1  5    0    1    0     1. SMALL INTERNAL RESISTANCE,
                                   E.G., .00001***
   VCCS1  3    0    4    0     1.
   VCG1   NL   0    4    0     1.
   DERIV1 4    5
```

Functionally Dependent Switching Characteristic (Actuated by Node Voltage Using Biased Limiters)

When the response variables are introduced into the standard NET-2 switch element, the solution simultaneity breaks down. Therefore, the following approach is useful for preserving simultaneity. A typical switching characteristic from low to high is shown in Figure 39 -- when the independent variable x (in this case, a node voltage) equals x_1, the value of y is switched from y_1 to y_2.

A simulation schematic is shown in Figure 39. The difference between the voltage x at node IN and the switching value x_1 at node 1 are

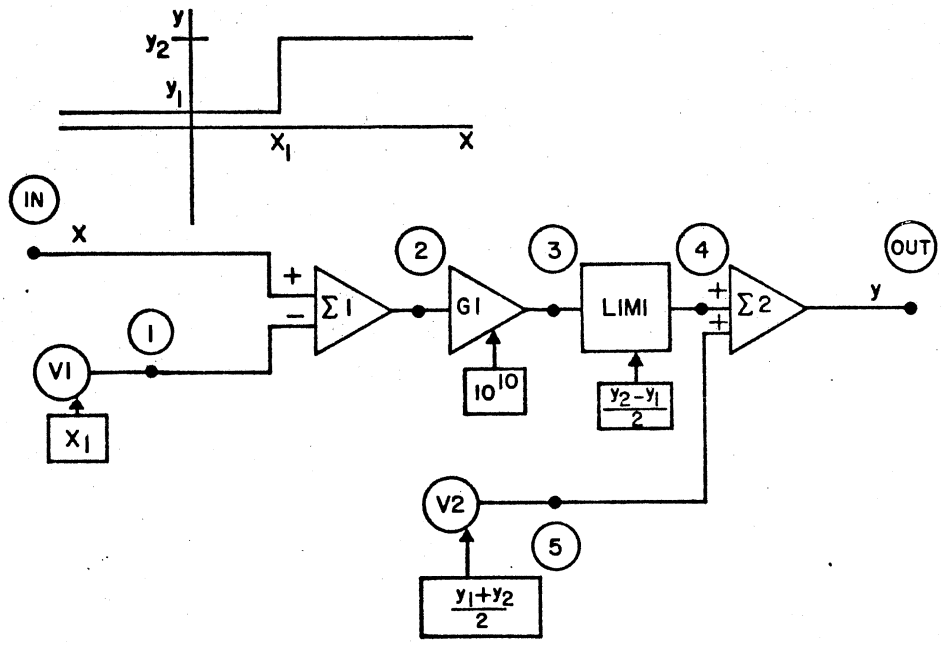

Figure 39. Functionally Dependent Switching Characteristic (Actuated by Node Voltage and Biased Limiters)

obtained in SUM1 at node 2. The difference $(x - x_1)$ is amplified with a high positive gain in GAIN1 and limited at $\pm (y_2 - y_1)/2$ in LIM1. Thus at node 4, y switches between $\pm (y_1 - y_2)/2$ at $x = x_1$. Then the level can be set by adding $(y_1 + y_2)/2$ at node 5 to node 4 in SUM2 to give the output at node OUT.

The NET-2 listing for this model, called SWITCH, is given in Figure 39 and Table XI. To switch from high to low, the slope is made negative either by performing the difference $(x_1 - x)$ or using a high negative gain in GAIN1.

TABLE XI

NET-2 LISTING FOR FUNCTIONALLY DEPENDENT SWITCHING CHARACTERISTIC

```
DEFINE     SWITCH      IN    OUT
    V1     1     0     ***VALUE OF X1***
    SUM1   2     +IN   -1
    GAIN1  2     3     ***HIGH GAIN, E.G., 10+10)***
    LIM1   3     4     ***VALUE OF (Y2-Y1)/2.***
    V2     5     0     ***VALUE OF (Y1+Y2)/2.***
    SUM2   OUT   +4    +5
```

VITA

Joseph Morton Iseman

Candidate for the Degree of

Doctor of Philosophy

Thesis: THE EVALUATION OF CIRCUIT MODELS OF LUMPED PASSIVE FLUIDIC COMPONENTS

Major Field: Mechanical Engineering

Biographical:

Personal Data: Born in Washington, D. C., July 18, 1939, the son of Mr. and Mrs. Issac Iseman; married to Sheila Cohen Iseman; father of two girls, Haylie Michelle (4 years) and Kerry Allison (2 years).

Education: Graduated from Calvin Coolidge High School, Washington, D. C., in June 1957; attended Harvard University from September, 1957 until June, 1958; attended George Washington University from September, 1958 until June, 1964; received Associate of Arts degree from George Washington University in October, 1959; received Bachelor of Science degree in Physics from George Washington University in October, 1961; attended The Catholic University of America from September, 1964 until June, 1969; received a degree of Master of Science in Engineering in Space Science and Applied Physics from The Catholic University of America in June, 1969; attended Oklahoma State University from September, 1969 to May, 1976; completed the requirements for the degree of Doctor of Philosophy in May, 1976.

Professional Experience: Physicist, Harry Diamond Laboratories, February, 1962 to present.

Member: ASME